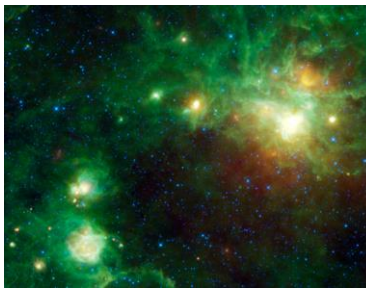

Massive Star Forming Regions at High Spatial Resolutions

Nuno Pinto de Carvalho
Mestrado Em Astronomia
Departamento de Física e Astronomia
2013

Orientador
M. S. Nanda Kumar, Doutor, Centro de Astrofísica da Universidade do Porto

U.PORTO

FACULDADE DE CIÊNCIAS
UNIVERSIDADE DO PORTO

Todas as correções determinadas pelo júri, e só essas, foram efetuadas.

O Presidente do Júri,

Porto, _____/_____/_____

Acknowledgements

I would like to thank my supervisor for the opportunity of working in the field of massive stars formation. I also would like to thank Lokesh K. Dewangan (Doutor, Centro de Astrofísica da Universidade do Porto) for his help in the initial data collection and analysis.

Abstract

Motivation: The processes involved in the formation of high mass OB stars are poorly understood.

Problem: Most luminous objects are far, highly extincted and resolving the details require high spatial resolution observations in the radio (mm) and infrared bands.

Observations: Adaptive optics imaging in the near-infrared, and diffraction limited imaging in the mid-infrared, both using VLT, of some of the most luminous sources have been analyzed. These observations probed into size scales of a few hundred to a few thousand AU, allowing us to examine the embedded stellar content and their environment.

With this spatial resolution, the best we've got so far, the objects are resolved as point sources with several details in circumstellar nebulae which are discussed here.

Keywords: Massive Stars; Star Formation; Adaptive Optics Imaging; Near-Infrared

Contents

List of Figures

List of Tables

List of Abbreviations

AO - Adaptive optics

CONICA - Coude Near Infrared Camera

ESO - European Southern Observatory

GMCs - Giant Molecular Clouds

H-R or **HRD** - Hertzsprung-Russell diagram. Graph showing the relationship between the stars absolute magnitudes/luminosities, with their spectral types, and the effective temperatures.

HC HII - High Compact HII

IR - Infra-red band

IRAF - Image Reduction and Analysis Facility (A general purpose software system for the reduction and analysis of astronomical data.)

IRAS - Infrared Astronomical Satellite. Regions of infrared radiation (heat energy) emitted from objects in the Universe

ISAAC - Infrared Spectrometer And Array Camera

ISM - Interstellar Medium

LGS - Laser Guide System

MS - Main Sequence in the HR diagram

MSX - Image archive (The Midcourse Space Experiment)

NACO - NAOS-CONICA

NAOS - Nasmyth Adaptive Optics System

PMS - Pre-main Sequence in the HR diagram

SED - Spectral energy distribution

SIMBAD - Set of Identifications, Measurements, and Bibliography for Astronomical Data (astronomical database http://simbad.u-strasbg.fr)

UC HII - Ultra Compact HII

UV - Ultra-violet

VLT - Very Large Telescope

WCS - World Coordinate System

YSO - Young Stellar Object(s)

1. Overview

The formation of stars and their evolution are very important to deepen our knowledge of the cosmos, as they are essential to the constitution of galaxies. Understanding these processes can be very difficult, but, without a doubt, it will give us a better view of the interstellar medium (ISM), galaxies, planetary formation, and of course, the universe evolution.

The theories that explain the formation of stars are physically very complex, and do not always correspond to the observations, thus being renewed from time to time. With the progress and development of new technologies for observation and study of these phenomena, especially in the (sub-)millimeter regime, interesting discoveries in the nearby (< 1kpc) star-forming regions have been made.

Star formation and stellar evolution are connected by a cycle of events known as the ISM cycle. A simplified description is: a star, born through collapse of a molecular cloud, looses mass in the form of strong stellar winds during most of its lifetime, until it reaches a critical point, where nuclear reactions can't sustain its weight and explodes, sending its remains back to the ISM. Part of the star's dust and gas can form new stars or become part of another molecular cloud.

Observations in our own galaxy show many stars of a wide range in luminosity. They are classified as stars of different size and mass, to better understand their formation and the physics involved (see: Table 1).

However, there are a number of unsolved problems in low and high mass star (and also planet) formation. In both low and high mass stars we start with an initial collapse of a rotating molecular cloud, but the differences begin to appear when we deeply analyze the physical properties of the cloud. Unlike low-mass stars, the accretion rates of the envelope ($\dot{M}$), for the high-mass, must be higher than for the low mass stars. This is a necessary condition to give the "star" more time to capture more mass. Massive stars begin to burn nuclear fuel even when accretion is going on, and the resulting radiation is powerful enough to stop further accretion creating a significant problem.

When the stellar core approaches the main-sequence (MS), the radiation, becoming stronger than the gravity, interacts with the dust in the infalling envelope. In the low-mass scenario, gravity always controls the infalling envelope.

The protostar evolution time is almost the same in the high and low mass cases, provided the accretion rate are different (higher for massive stars). This is consistent with some observations, indicating that massive stars form in very turbulent and

dense environment ($n = 10^6 cm^{-3}$) (see: Bodenheimer, P. H., 2011, p.184 and Lada, C.J., Lada, E.A., 2003). We will further discuss these time scales and compare them for the low and high mass stars.

Stars	Mass
Low mass	< 3 $M_\odot$
Intermediate	3 - 8 $M_\odot$
Massive	> 8 $M_\odot$

Table 1 - Stars mass classification [1]

Stars can form in small groups, massive clusters and associations, or in isolation. Based on many observations, it is more common to find low-mass stars whose formation can be traced back to small clusters, populated with a few hundred objects (see: Lada, C.J., Lada, E.A., 2003). Massive stars form along with many of these low mass stars, probably with similar conditions in molecular clouds. (see: Bodenheimer, P. H., 2011, p.184)

In this work we will focus only on massive star formation, which is less understood. The detailed study of the work that has been made by other authors and published over the years will facilitate the analysis of the luminous IRAS sources selected here, which are presumably good candidates for massive young stars (see: Krumholz et al. 2009, Kuiper et al. 2012, Cunningham et al. 2011). We will look for interesting structures that could help examine the embedded stellar content and tell us something about their environment. For this study we have to understand the difference between the low and high mass regime.

A star is considered massive when its mass is, at least, eight times greater than that of the Sun. There are many problems regarding these stars size and mass. Although a number of factors tend to limit the star's size, many massive stars have been observed in the past few decades, and some can go up to 150 times the size of our Sun, at least theoretically (see section: 1.1. Eddington Size Limit). Therefore, it is necessary to understand the basic conditions in which massive stars form. We know that stars form due to the gravitational collapse of dense molecular clouds of interstellar gas. As the gravitational pull increases with the accretion of mass, the "star" (protostar) produces stronger radiation pressure, as a result of Kelvin-

[1] We can't have stars with less than 0.08 $M_\odot$ because there isn't sufficient mass to start nuclear reactions in the core. Depending on different books, massive stars have a minimum of 8 to 10 solar masses.

Helmholtz contraction and the nuclear reactions in the core. The radiation pressure limits the stars size, because it will blow away the surrounding gas that would eventually be accreted onto the star. However, recent studies (see: Bodenheimer, P. H., 2011, p.206) show some important effects, for instance, the formation of a radiation bubble (discussed at the end of the section: 2. Massive Star Formation and Location), through which radiation is dissipated, allowing the accretion of gas to continue, for the massive stars. This is an important step because, according to the most realistic simulations obtained so far, the material can continue to infall onto the disk, because the strong radiation pressure escapes in the outflow cavity.

There are some observation related problems we face when studying these stars. In the process of formation, massive stars can be very bright and luminous, but they are relatively few in number, located very far in our galaxy, at large distances from us (limiting our spatial resolution), associated with clusters (problem in resolving individual objects), in regions very obscured in optical radiation, being highly extincted. So, to study these massive stars we require high spatial resolution observations in the radio(mm) and infrared bands, so we can resolve their details. The radiation that we detect, in the near IR, comes from the heated dust and gas surrounding the stellar core. This is the only way to detect the early stages of a star's life and its embedded content, because the infrared light (heat) penetrates the dust more easily than the visible light. The extinction (absorption and scattering of radiation) caused by the surrounding stellar cloud of gas and dust is too high to let us observe the details in the visual bands.

To proceed with the study of massive stars, some of the most luminous sources have been selected (see: Faúndez et al., 2004). They were recently observed using adaptive optics imaging in the near-infrared and diffraction limited imaging in the mid-infrared, both using some powerful instruments of the Very Large Telescope, that we will explain further. Here, those observations are reduced and analysed.
The data include 21 luminous IRAS sources, which are nearby (1kpc to 4kpc from us). The data for these sources, in the Ks band, was downloaded from the ESO Archive website (http://archive.eso.org/eso/eso_archive_main.html) only for VLT/NACO instrument imaging. The Ks band was chosen because it allows to probe deeper into the stellar content (2.2 micron wavelength range, NIR). Using the program IRAF (Image Reduction and Analysis Facility, software for the reduction and analysis of astronomical data, available at http://iraf.noao.edu) the data for each source was reduced by sky-subtraction and mosaicking. The resulting images were

analyzed using SAOImage DS9 (an astronomical imaging and data visualization application, available at http://hea-www.harvard.edu/RD/ds9/site/Home.html), to look for nebular structures around the sources. Eight sources show significant structures which are further examined and compared with the data in the literature.

A detailed research of published literature, for each IRAS source, was made throughout SIMBAD Astronomical Database (http://simbad.u-strasbg.fr). Identified structures are associated with Ultra Compact HII regions (UC HII), which are regions of ionized gas (densities range from 10^6 particles per cm^{-3} to just a few particles per cm^{-3} and masses from 100 to 10^6 $M_\odot$), which are elaborated for each source.

1.1. Eddington Size Limit

Eddington Limit, or Eddington Luminosity, found in some books and articles, refers to the point where the luminosity or radiation, emitted by star in formation (still accreting matter), becomes so strong that the forming star starts expelling the outer layers of matter.

High mass stars have a higher rate of core energy production, so, the luminosity increase exceeds the mass proportion (Bodenheimer, P. H., 2011, p.206). This mass-luminosity[2] relation is approximately of the form $L \propto M^{\alpha}$, where $\alpha = 3.5$ for main sequence stars with masses between 2 and 20 solar masses (see: Shu, F. H. 1982, p.146 and Salaris, M., Cassisi, S., 2005, p.138).

The outward pressure of radiant energy is a combination of Kelvin-Helmholtz contraction and nuclear fusion, in the case of massive young stars, and exceeds the inward pull of the gravity. Surpassing this limit means that a more massive star would rip itself apart or would loose mass at a very high rate, shedding mass into the surrounding space, under strong stellar winds of radiation, reducing its internal energy production to a lower and maintainable rate.

The upper limit for the mass (Eddington limit) is established by the radiation pressure in the star's photosphere. Based on the above formula, a small increase in solar mass translates in a much higher luminosity than the Sun. An $80M_{\odot}$ star would have more than 100 times the Sun's luminosity.

Initial Solar Mass ($M_{\odot}$)	Lifetime in MS (Myr)
0.5	56000
1	12000
2	900
5	90
20	6
40	0.5

Table 2 - Initial Solar Mass vs. Lifetime in MS

[2] Luminosity is what determines if a star is massive or not. Assuming a star behaves as a black body, good approximation, the luminosity, L, is related to the temperature, T, and radius, R, of the star. The mass-luminosity relation is determined using and comparing other known stars, in which their distances were calculated through reliable techniques.

If any star exists above 150-200$M_{\odot}$, the theories of stellar evolution needs to be changed, because a more massive star should have a very short life (see: Table 2, and http://spiff.rit.edu/classes/phys230/lectures/star_age/star_age.html). The most massive stars found today are O2 type stars.

1.2. Kelvin-Helmholtz Contraction Timescale

The Kelvin-Helmholtz time scale, also called thermal time scale, is the time scale in which the star would radiate its energy away by converting all the potential energy into radiation through contraction, in the pre-main sequence phase:

$t_{kh} = \frac{3}{10} \times \frac{GM^2}{RL}$ (where G is the gravitational constant; M is the star's mass; R its radius and L its luminosity),

This time scale, along with the accretion rate $\dot{M}$ and the accretion time: $\frac{M}{\dot{M}}$,

Can differentiate the high and low mass star formation processes.

- For low mass stars:

$t_{kh} = 3 \times 10^7 \, yr$ $\quad \dot{M} = \frac{1}{3} \cdot 10^{-5} M_{Sun} / yrs$ $\quad M / \dot{M} = 3 \times 10^5 \, yrs$ (for $1M_{\odot}$)

- For high mass stars:

$t_{kh} = 3 \times 10^4 \, yr$ $\quad \dot{M} = 5 \times 10^{-4} M_{Sun} / yrs$ $\quad M / \dot{M} = 10^5 \, yrs$ (for $50M_{\odot}$)

Moreover, for high mass stars the accretion rate will also result in a large amount of radiation growing due to the $\frac{GM^2}{RL}$ factor (see: Bodenheimer, P. H., 2011 p.183-184).

2. Massive Star Formation and Location

Massive stars in our galaxy are born inside high density cores of giant molecular clouds, and have spectral classes O and B (see: Table 3), often located in groups, called OB associations. They live for very short time, burning their hydrogen so fast, that they are the first to leave the main sequence, and don't move very far from their birth location.

During their initial life, they emit large quantities of UV radiation that rapidly start ionizing the dense molecular gas, creating an HII region. "This most visible manifestation of massive star formation begins when the Lyman continuum output from the massive young stellar object becomes sufficient to ionize the surroundings from which it was born" (see: Hoare, M. G. et al. 2006). Also, the circumstellar dust that surrounds the ionized gas absorbs most of the star's radiation (directly or processed through the dense gas), formatting compact regions of heated dust that reemits the radiation in the far-infrared of the spectrum. This compact region is commonly classified as an ultra compact HII region (UC HII) (see: Garay, G., Lizano, S. 1999). The study of such regions will allow us to learn about the newly formed massive stars.

Spectral Class	Fraction of MS	Temperature (K)	Luminosity ($L_{\odot}$)
O	0.00003%	33.000 - 60.000	>30.000
B	0.13%	10.000 - 33.000	25-30.000

Table 3 - Massive stars spectral type characteristics
(This info is available at multiple websites and books. Please see the references.)

Two theoretical scenarios, namely core accretion and coalescence, try to explain the formation of massive stars, although it is not clear how the actual formation takes place.

In the core accretion, we have the low-mass star formation extended to the high-mass stars. Massive stellar objects can be formed through similar accretion based process as the low-mass counterparts, but with much higher accretion rates (see: Yorke & Sonnhalter 2002, and section: 1.2. Kelvin-Helmholtz Contraction Timescale)

According to coalescence[3], massive stars could form at the center of very dense clusters, through mergers of intermediate-mass protostars. (see Stahler et al. 2000, Bally 2002)

[3] You can also find cohesion instead of coalescence in the literature mentioned (see: References).

It “has been proposed that massive stars form through a process of coalescence of low mass stars or protostars (e.g. Bonnell et al. 1998) or through a process of “competitive accretion” (e.g. Bonnell et al. 2001; Bonnell & Bate 2006) within the cluster.” (see: De Buizer, J. M., et al. 2009). Some recent models indicates that massive star formation, according to theory, is very similar to low mass star formation but “in a scaled-up version” through core accretion onto the disks (see: McKee & Tan 2002, 2003; Krumholz et al. 2005b, Krumholz et al. 2005c). Accretion disks haven’t been observed directly, but they solve many conflicts on how the mass transport is made onto the O and B star.

Regardless of which scenario is at work, it is believed that formation of massive star requires high column density in molecular cloud cores ($\Sigma = \frac{M}{\pi R^2}$), than the required for low mass stars. For example, a star with 100$M_\odot$ require $\Sigma = 0.7\ g \cdot cm^{-2}$ whereas a 1$M_\odot$ require $\Sigma = 0.027\ g \cdot cm^{-2}$ (see: Bodenheimer, P. H., 2011, p.188-189).

Massive stars are studied by observing:
1. Gravitationally bound OB clusters
2. OB associations (between 1pc and 10pc apart)
3. Individual OB stars that were ejected from a cluster (with velocities of 40Km/s or more)
4. Massive OB that can’t be traced back to an original cluster or association (group) and may have formed independently (< 10% of all massive stars observed).
(see: Bodenheimer, P. H., 2011, p.184)
Massive stars with M > 10 $M_\odot$ are few in number, and are located in regions highly obscured in optical radiation, so we observe at longer wavelength, such as radio, far-infrared and some near-infrared (L and Ks bands, 3.3μm and 2.2μm), indirectly, from the heated dust and gas around the star. The dust and gas absorbs and re-emits the star radiation.
One of the sign-posts of a forming star is the presence of bipolar outflows, continuous flows of gas from the polar region. Observations show that are associated with massive stars and also low mass stars (see: Bodenheimer, P. H., 2011, p.188). This may indicate that the massive star is accumulating material from the surrounding cloud through an accretion disk, similar to the process known for low

mass stars (see: Garay, G., Lizano, S. 1999). Indirect evidence for the massive stars accretion disks is increasing.

There are some relevant problems, which still need to be mentioned, when studying young massive stars. The most common and very important aspect for their formation is the effect of radiation pressure that we referred earlier in the Overview. The radiation pressure may block the accretion processes when the star's mass reaches around $10M_{\odot}$. The book Principles of Star Formation, by Bodenheimer, P. H., 2011, states that "massive stars form from massive cores, and that mergers play only a minor role" (see: Bodenheimer, P. H., 2011, p.204), after some numerical 3D simulations being considered (see: Figure 1). When the star in the simulation reached about $17M_{\odot}$, the radiation effects became a very important part of the mechanics and the outflow of the star, so that the gas started being expelled in the polar direction (see: Krumholz et al. 2009). The radiation started to form a bubble, restricting the flux of material (gas and dust), above and below the equatorial plane.
At this moment of the simulation, things started to get very interesting, because it seems to contradict some of the ideas and physics about the strong radiation pressure blocking the continuing accretion of mass. The infalling gas hit the boundary of the bubble and travels along its surface until it reaches disk, where the radiation is much more week. This important fact allow the continue accretion of matter for stars with much more mass than 10 $M_{\odot}$. Other different effects, not included in the theoretical simulations, could also be favorable to accretion, like the frequency-dependent transfer of radiation, the presence of outflows, reducing the radiation pressure in the pole direction and the presence of magnetic fields, introducing another instability, but that helps the formation of dense regions of gas that move inward, while radiation escapes through low dense regions (see: Bodenheimer, P. H., 2011, p.106, and Krumholz et al. 2009).
We can sate that, although not all effects were included in the simulations, we have a considerable number of reasons that supports the further accretion, for stars with >10 $M_{\odot}$, breaking the radiation barrier and leading to the formation of a massive star.

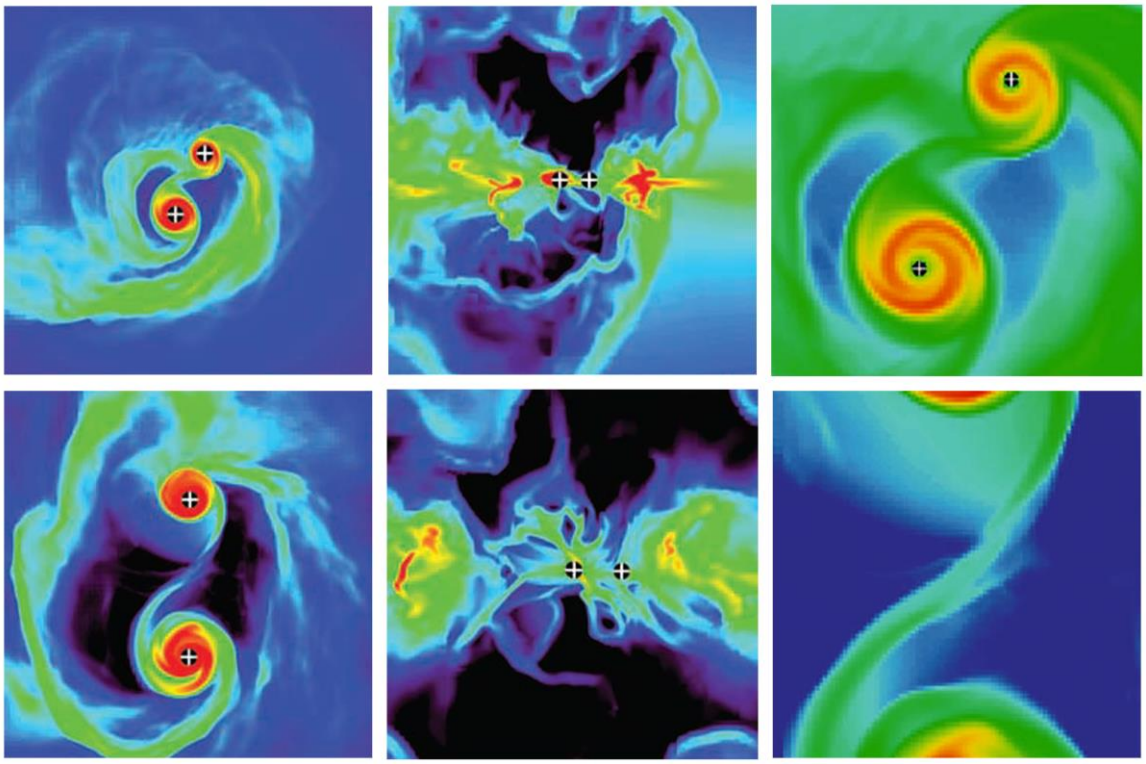

Figure 1 - Numerical 3D simulation.
Formation of stars with masses greater than 20 solar masses. Stars are indicated by crosses. Upper images correspond to a time 41.7 kyr, and lower images to 55.9 kyr. Logarithmic color scale indicates the column density in a plane perpendicular to the rotation axis, with a range from 10^{-1} (dark blue) to 10^{3} (orange) g cm^{-2}. Box size is 966 AU in the right panels and 3,864 AU in the left and center panels.
"The generation of a massive binary is evident; note circumstellar disks as well as circumbinary material. The orbit expands with time and reaches a semimajor axis of 1,280 AU at the end of the simulation." From Krumholz et al., Science 323, 754 (2009), and Bodenheimer, P. H., 2011, p205. Reprinted with permission from AAAS.

As we referred in the overview, young massive stars are associated with Ultra Compact HII regions (UC HII), but we can also find some earlier phases prior to the formation of UC HII (they are sites of methanol maser emission, see section: 2.1. Maser Emission).

Many massive young stellar objects (YSOs) were found scattered across the Galactic Plane, based on surveys of CH3COH (Methanol) emission (see: Norris et al. 1998, Walsh et al. 1998). The studies that followed after these surveys (see: Minier et al. 2003, Walsh et al. 2003, Ellingsen 2006), came to confirm that “methanol masers are reliable indicators of massive star formation” (see: De Buizer, J. M., et al. 2009) and as the UC HII region develops through time, the maser activity may fade out.

This concludes that methanol masers not only trace massive star formation, as it indicates its earliest stages, where the new formed stars may be dominated by accretion (see: Walsh et al. 1998, Roman-Lopes et al. 2003).

Other important thing to note is that UCHII regions have spectral energy distributions in the far infra-red (see: Wood & Churchwell 1989), with spectral densities greater than 10^{4} cm^{-3} and diameters smaller than 0.1pc (see: Roman-Lopes et al. 2003). This

gives us an idea of the size scales we are dealing with, and resolution needed, when studding dense stellar cores (with single sources/stars and their environment resolved).

2.1. Maser Emission

A laser emits radiation/light, amplified through the process of stimulated emission of radiation/photons. (LASER - Light Amplification by Stimulated Emission of Radiation)
In stimulated emission, a photon is fired onto an atom, already in its high energy state from a prior absorption. The atom absorbs the photon, but quickly emits two photons of the same wavelength of the first photon to get back to its original, lower and stable energy state. This happens because atoms absorb photons of the right "size", but don't like to stay in high energy states, according to quantum mechanics.
In this scenario, we have a "snowball effect", where each photon stimulates emission from the next molecule in a chain, doubling the number of photons in each process.
A laser has a high degree of spatial (and temporal) coherence, with an appearance of a narrow and concentrated beam of light. Spatial coherence is the same correlation observed in different points in space, and temporal coherence is the same correlation observed in different moments in time (see: Born, M., Wolf, E., 1999).

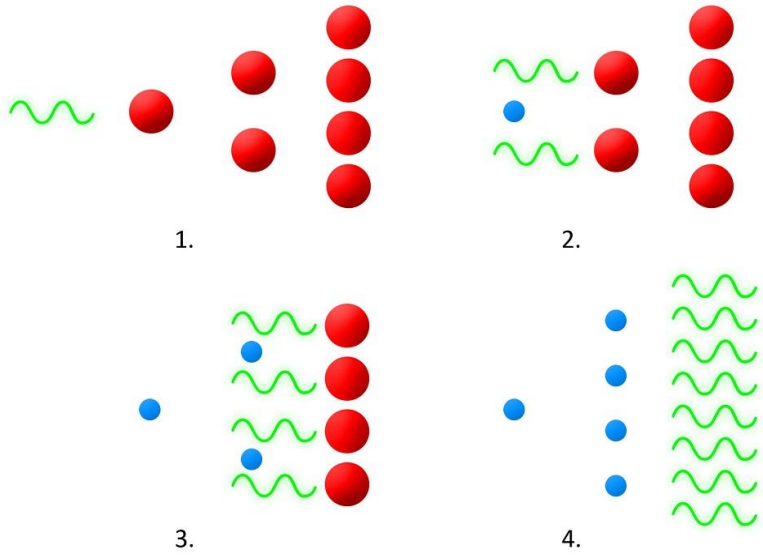

Figure 2 - Maser emission
A photon (green wave) interacts with an atom in its high energy state (represented by a red circle). The atom absorbs the photon and emits two photons of the same frequency, going to its lower energy state (blue circle). The process repeats from 1. to 4, always doubling the initial number of photons.
(Image based on the one found at http://einstein.stanford.edu/content/faqs/maser.html)

According to a maser, the effect described is the same, but for microwave radiation (MASER - Microwave Amplification by Stimulated Emission of Radiation) (see: Kutner, M. L., 2003, p280, http://einstein.stanford.edu/content/faqs/maser.html, and Figure 2).

Our Sun’s radiation, for example, can’t produce a maser because it lacks spatial coherence. It requires for the medium, or gain medium, to have a substantial and approximately constant number of molecules, so it can maintain a good coherence in the component of the velocity along the line-of-sight. The dense environments of massive stars, which we talked about in the above sections, are favorable mediums for maser propagation.

3. Work Carried Out

We studied and analyzed images obtained by 8.2m Very Large Telescope (VLT) operated by European Southern Observatory (ESO). NACO (NAOS-CONICA, NAOS stands for: Nasmyth Adaptive Optics System and CONICA: Coude Near Infrared Camera) is an instrument of the VLT (VLT/NACO) that provide adaptive optics imaging, imaging polarimetry, coronography and spectroscopy, in the 1-5 microns range. NACO has the ability to produce very high resolution infrared images, the kind of images we need to study the small details of high mass stars (see: http://www.eso.org/sci/facilities/paranal/instruments/naco).

Adaptive optics (AO) is a system used to improve performance by reducing the wave-front distortions effect (blurred image), caused by Earth's turbulent atmosphere. This technology provides sharper images, and an additional contrast gain, so that fainter objects can now be detected. This system uses a star to calibrate and deforms a small mirror to correct the distortions. The corrections takes place in a matter of milliseconds, faster than the atmosphere can change.

Since adaptive optics needs a nearby reference, a bright star to be used as a guide, it limits the area of the sky to be observed, because there aren't sufficient bright stars available in all parts of the sky. To compensate this problem, there is another technology, Laser Guide System (LGS), involving a powerful laser that creates a fake guide star, so that its variations through time can be measured and corrected, reducing the atmospheric distortions of light. There are two main types, Sodium and Rayleigh guide stars. Sodium laser, tuned to 589.2 nanometers, is used to energize a layer of sodium atoms in the mesosphere (layer with an altitude of ~19Km). This region will re-emit the light, creating the effect of a star. On the other hand, Rayleigh guide stars are produced by a laser, near UV, and detecting the scattering of light by the molecules in a lower atmosphere (15-25Km). This second is less expensive, but doesn't give a good wave-front reference due to the fact the artificial light is generated in a much lower altitude, thus part of the scatter radiation, at ground level, is ignored.

4. Data Reduction and Analysis

In this work we analyzed 21 IRAS regions, selected from Faúndez et al. (2004) (see: Faúndez et al., 2004), based on luminosity and distance. All targets were selected for distances below 5kpc, except the last one (see: Table 4). The last source in the table was selected because it showed a very high luminosity for a source that is at 7.0kpc from us.

RAJ2000	DEJ2000	IRAS	Dist (kpc)	Lum ($L_{\odot}$)
135.47598	-47.73355	09002-4732	1.2	39000.
260.22318	-35.78349	17175-3544	1.5	78000.
256.09326	-40.74168	17008-4040	2.0	52000.
272.71279	-17.92790	18079-1756	2.4	20000.
238.95179	-52.71981	15520-5234	2.9	200000.
276.42646	-13.17170	18228-1312	3.0	59000.
245.38538	-50.42169	16177-5018	3.4	340000.
245.04603	-50.88561	16164-5046	3.7	400000.
232.33470	-56.52481	15254-5621	4.4	120000.
241.90862	-52.51430	16037-5223	4.9	110000.
197.80155	-62.57747	13079-6218	4.9	280000.
249.70754	-47.46777	16351-4722	3.20	9.3e+04
253.13961	-44.60557	16489-4431	3.40	1.5e+04
254.01078	-43.08162	16524-4300	3.60	4.2e+04
245.25766	-50.59265	16172-5028	3.50	4.4e+05
241.60586	-50.72246	16026-5035	4.80	1.4e+05
239.03472	-54.33148	15522-5411	3.10	2.1e+04
188.89117	-63.04371	12326-6245	4.40	2.7e+05
093.3680	+17.92480	06105+1756	3.38	1.6e+04
283.4089	+1.840900	18511+0146	3.86	2.0e+04
240.1367	-52.7460	15567-5236	7.0	8.0e+05

Table 4 - List of IRAS sources

4.1. Collecting the Data

For downloading the image data-packs we had to insert the source target name (SIMBAD name), for each IRAS region, in the ESO data archive website, http://archive.eso.org/wdb/wdb/eso/naco/form only for VLT/NACO instrument, and select the Ks band imaging filter in the instrument specific information. A list with all the datasets from the NACO query results was obtained, for a specific IRAS region. This list contains the info on each data set, being the object or a sky-frame. (The object and sky frame name/info was stored in a TXT file, so that, when analyzing the each data set, we know which file we are dealing with, for latter treatment/analysis) We selected all the objects and sky-frames for request submission. Finally, when available, the data-pack for each IRAS region was downloaded and treated one by one.

The downloaded data-sets were decompressed and analyzed in a Linux operating system, through inputted commands in a terminal window, using IRAF (available at http://iraf.noao.edu) in a separated xgterm window, and using SAOImage DS9 (available at http://hea-www.harvard.edu/RD/ds9/site/Home.html).

4.2. Data Reduction

Data Reduction procedure involves the subtraction of the sky in each object and combining the resulted images of the object. This is an important step because infra-red images have a very bright sky/background that covers the low level emission from the actual object.

Since each image as an exposure time, by combining many images we are adding all the exposure times and decreasing the background noise. This will also improve the signal/noise ratio.

After downloading the data, for a certain IRAS region, the images were decompressed (command: `gunzip *.z`), and to be sure there weren't any errors or corrupted images the IRAF command "imstat" was used (exemple: `imstat *.fits[0]`) along with imheader command (exemple: `imheader *.fits[0]`) to check each *.fits" file or image.

A proper sky-frame for each object was chosen, by looking for a sky whose position is similar to the source (revealed by its file name), and than subtracted. This was made for every object (example: `imarith <object>.fits[0] - <sky>.fits[0] <result>`).

The subtracted images were checked in the SAOImage DS9 (“zMax” and “log” scale parameters selected) and compared in WCS (World Coordinate System) (in DS9, Tab Frame > Match > Frame > wcs). Images with a very different wcs were treated separately to avoid elongation (stretch effect) in the final result(s) image.
The sky subtracted images of each exposure was combined to produce a final mosaic by using the command “imcombine”.

Before using the “imcombine” command in IRAF, to combine the images, some parameters were changed. Using “epar imcombine” we accessed its parameters:

```
>input= @<filenames>.txt
>combine=median
>offsets=wcs
>scale=median
```

This is necessary to correctly align all the images when combining. After combining the images we checked the result in DS9 for errors.

The above steps were made to all of the IRAS regions, to obtain a final good quality image of the source. Now we shall proceed with the study in detail and look for relevant structures for all combined sources (see: Figure 3).

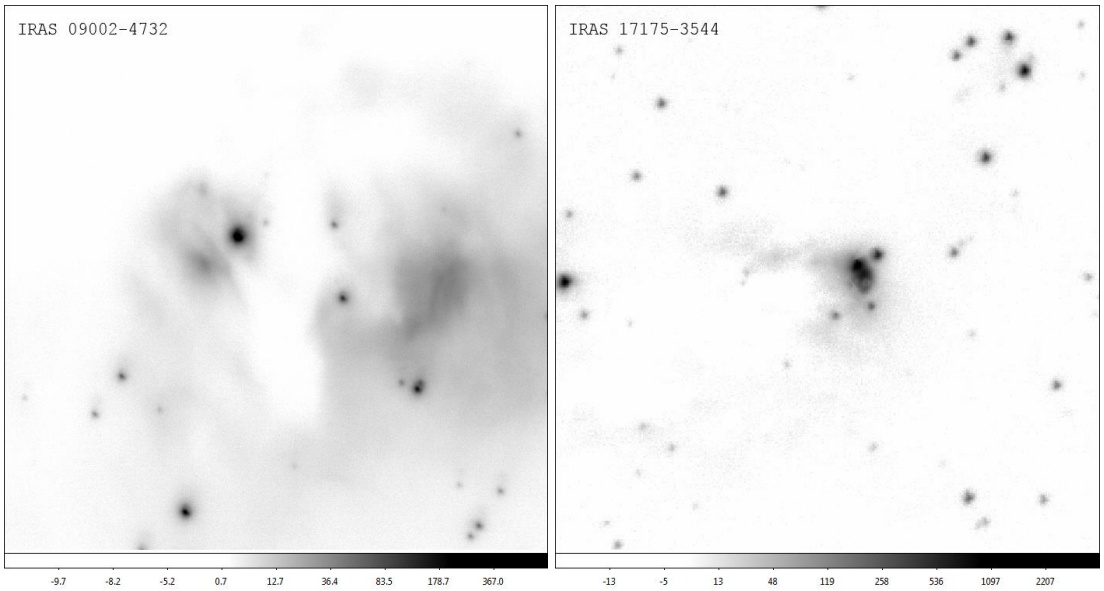

Figure 3 (.1), (.2) - Combined IRAS sources
The left panel, (.1), has the size of 0.3’ x 0.3’ and the right panel, (.2), 0.4’ x 0.4’.

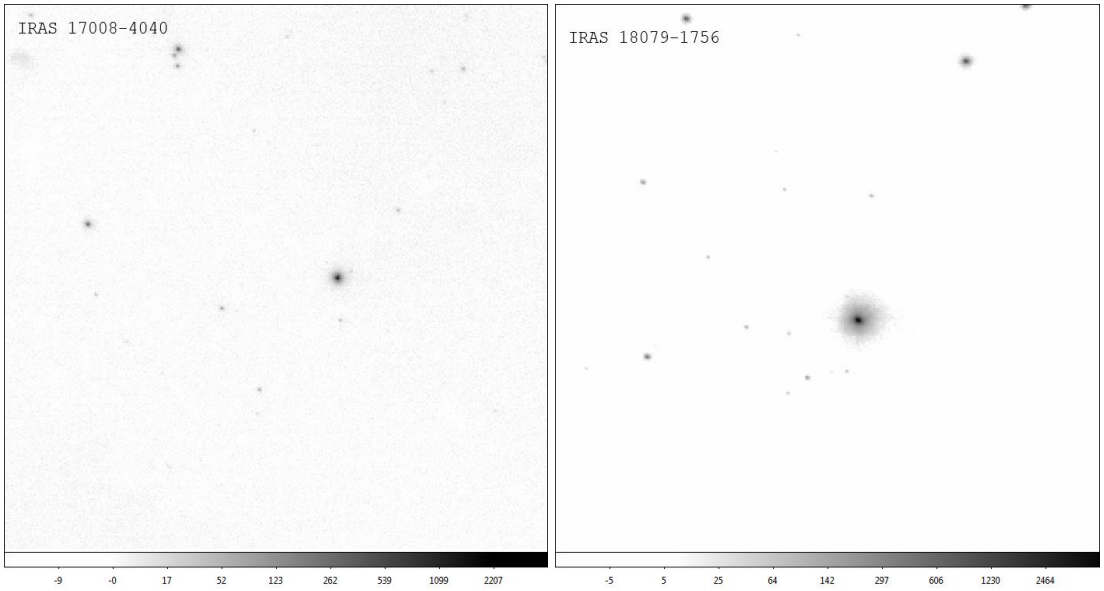

Figure 3 (.3), (.4) - Combined IRAS sources
The left panel has the size of 0.4' x 0.4' and the right panel 0.3' x 0.3'.

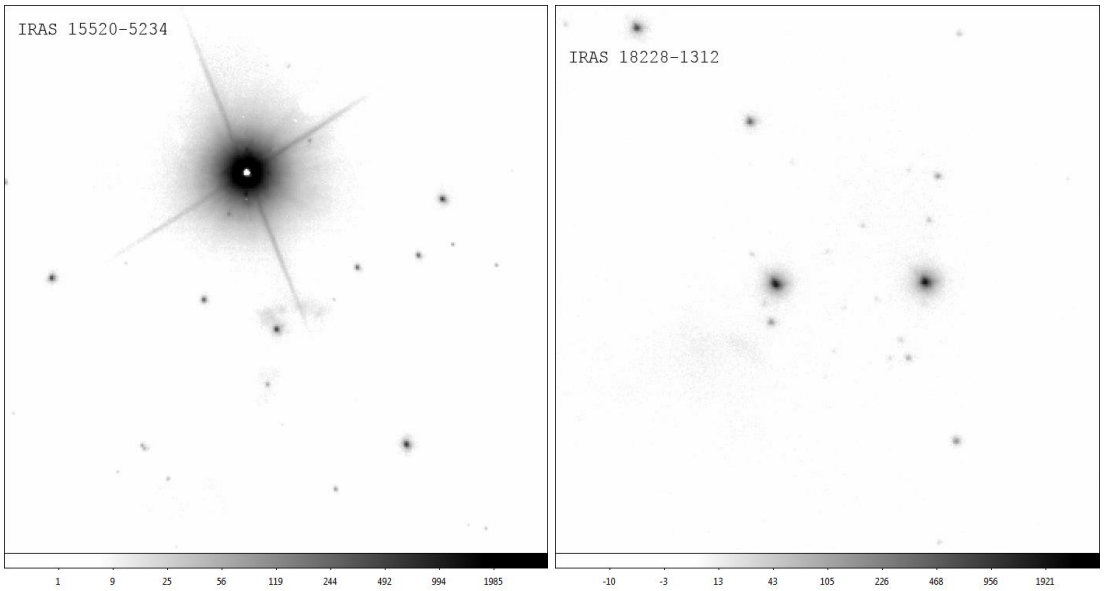

Figure 3 (.5), (.6) - Combined IRAS sources
Left and right panels have the size of 0.3' x 0.3'.

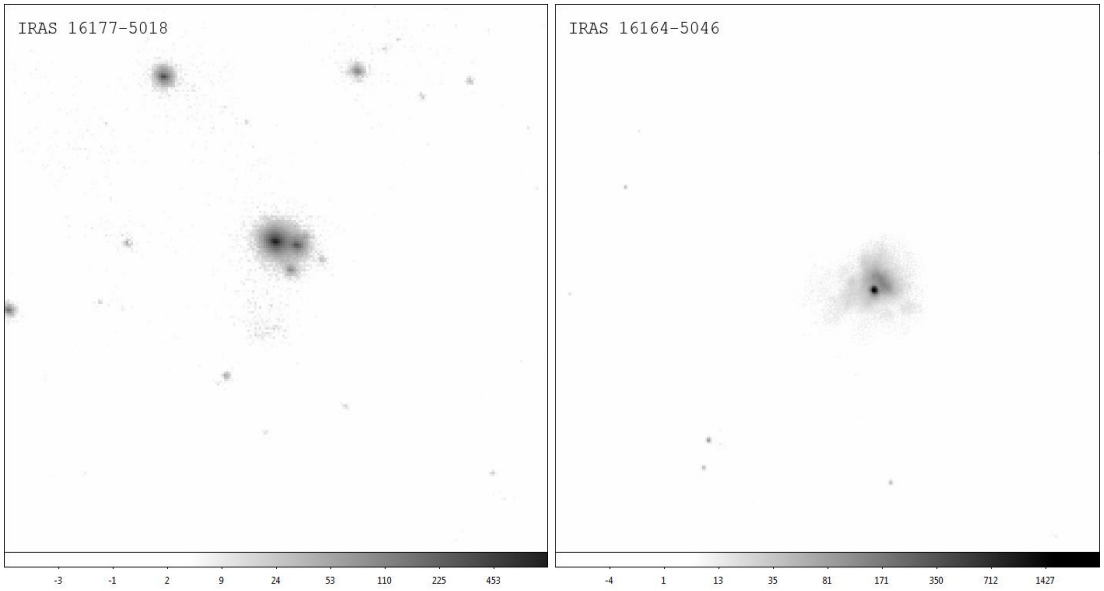

Figure 3 (.7), (.8) - Combined IRAS sources
The left panel has the size of 0.2' x 0.2' and the right panel 0.3' x 0.3'.

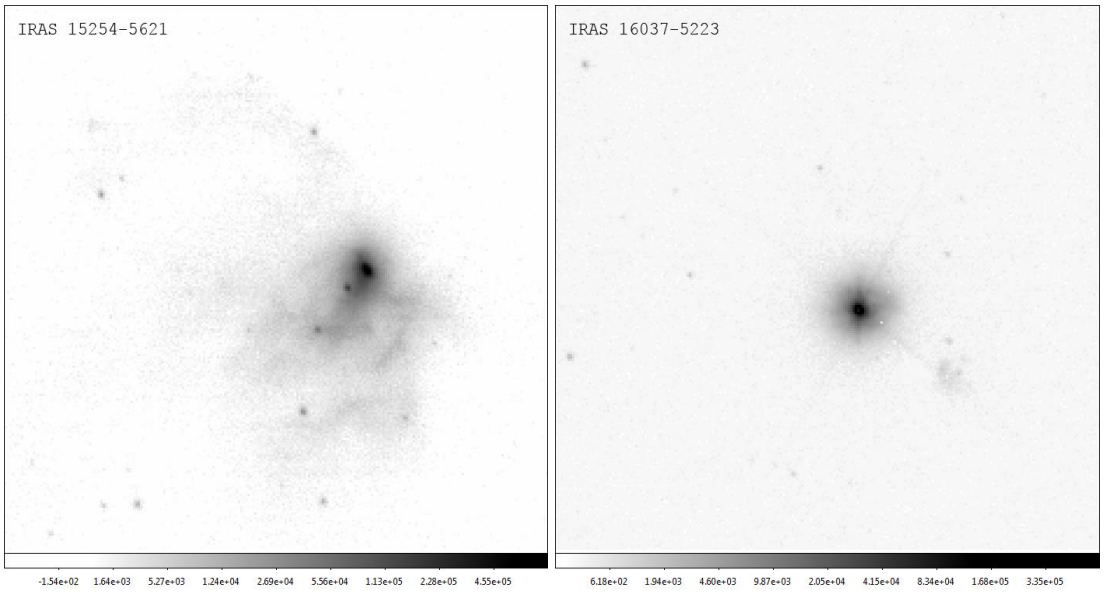

Figure 3 (.9), (.10) - Combined IRAS sources
Left and right panels have the size of 0.2' x 0.2'.

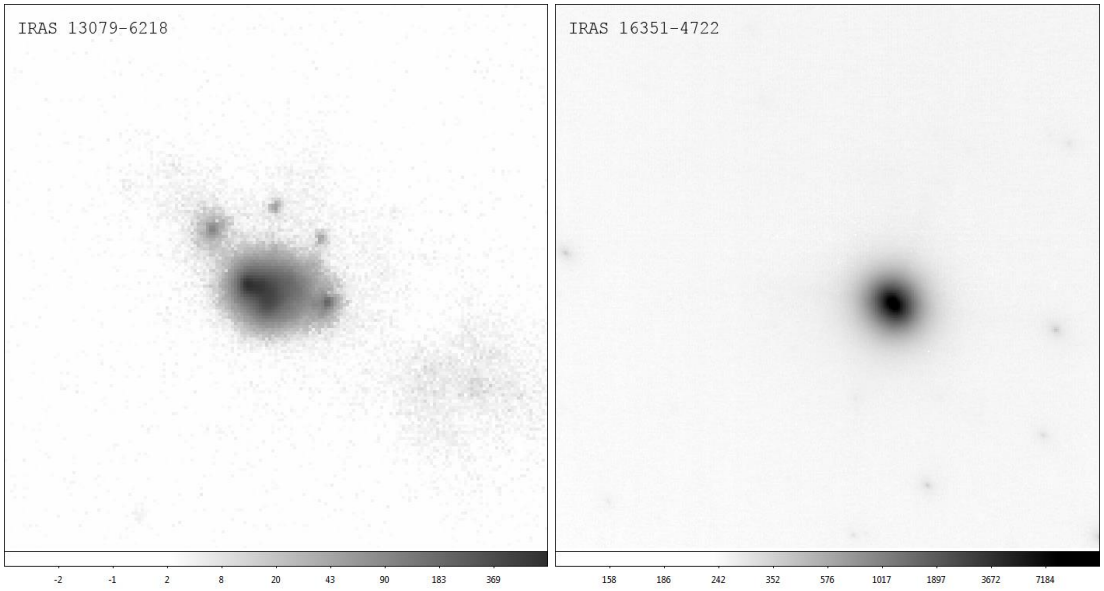

Figure 3 (.11), (.12) - Combined IRAS sources
The left panel has the size of 0.15’ x 0.15’ and the right panel 0.3’ x 0.3’.

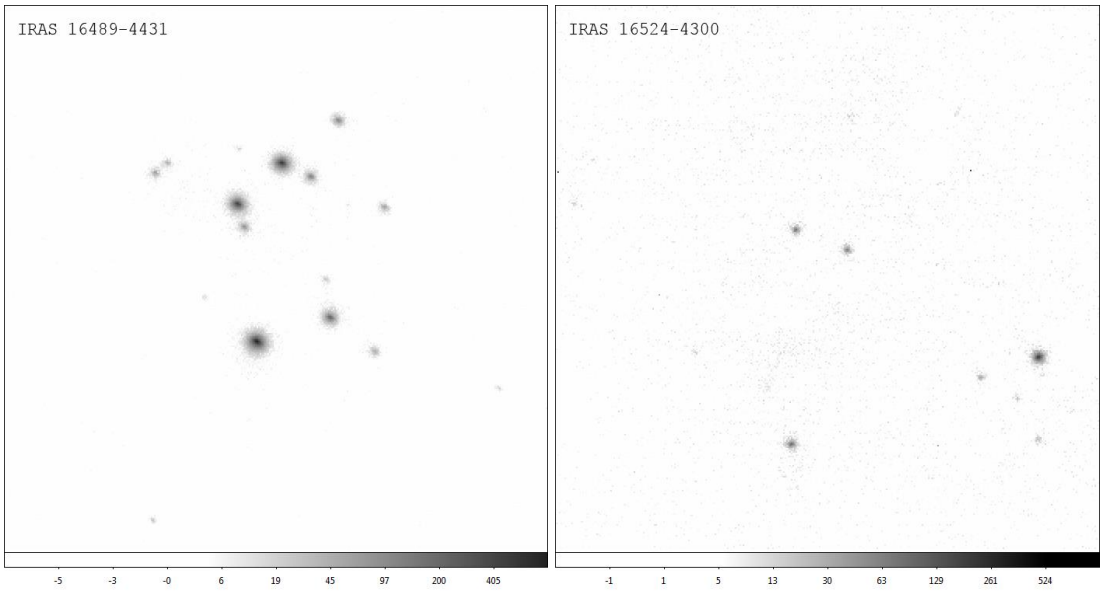

Figure 3 (.13), (.14) - Combined IRAS sources
Left and right panels have the size of 0.3’ x 0.3’.

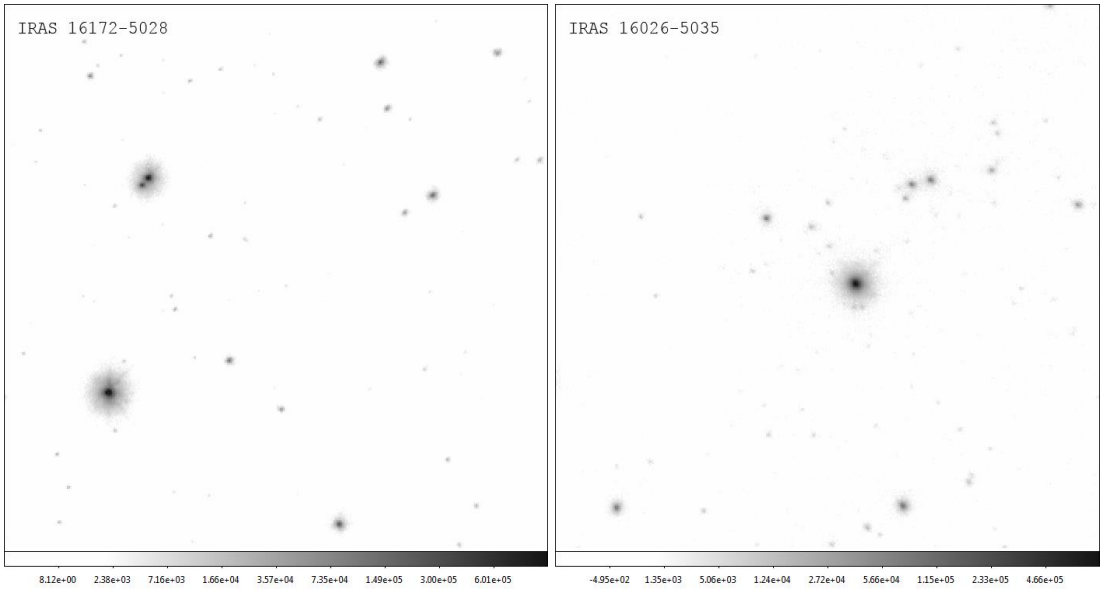

Figure 3 (.15), (.16) - Combined IRAS sources
Left and right panels have the size of 0.3' x 0.3'.

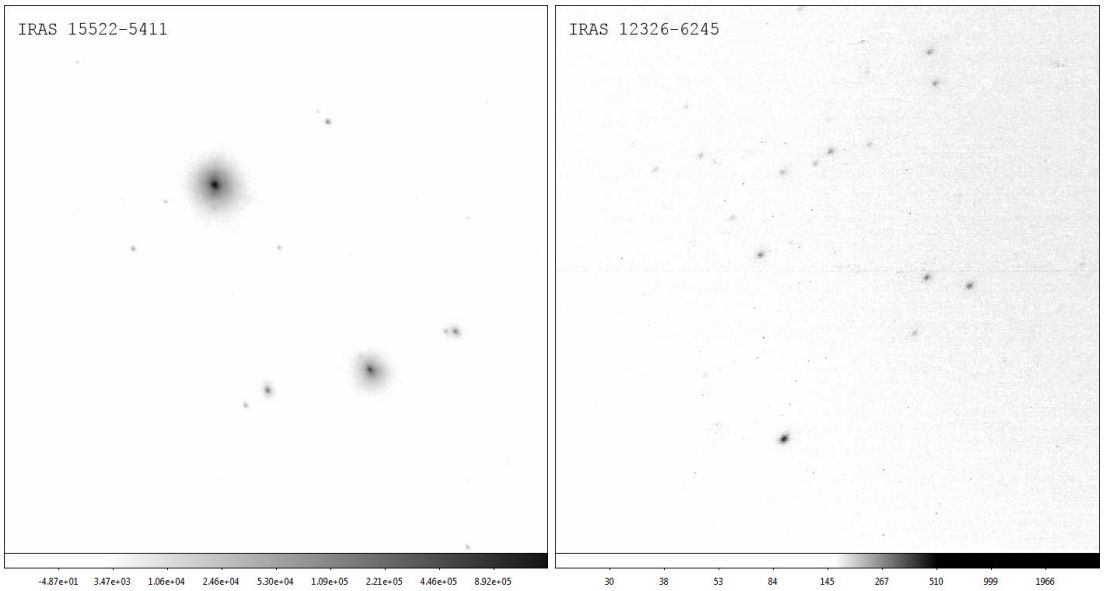

Figure 3 (.17), (.18) - Combined IRAS sources
Left and right panels have the size of 0.3' x 0.3'.

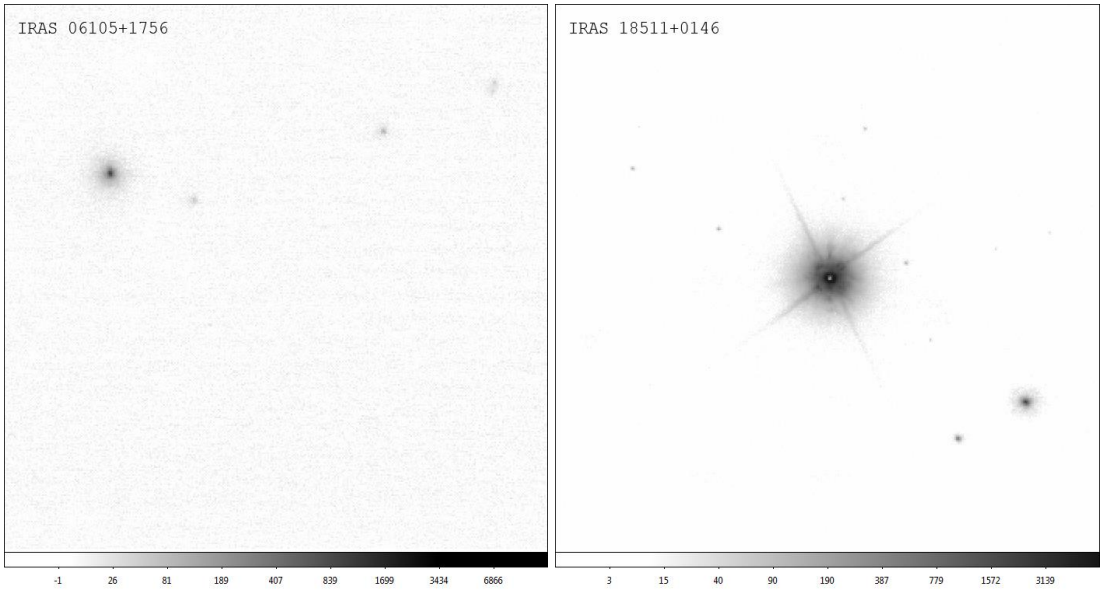

Figure 3 (.19), (.20) - Combined IRAS sources
The left panel has the size of 0.15’ x 0.15’ and the right panel 0.3’ x 0.3’.

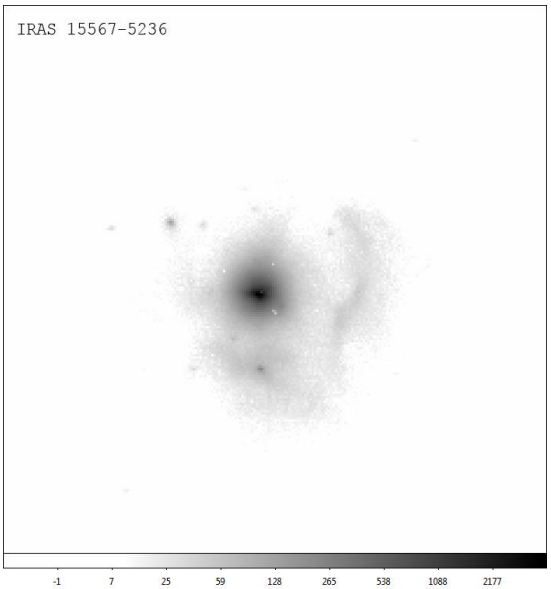

Figure 3 - Combined IRAS sources
This panel (.21) has the size of 0.2’ x 0.2’.

4.3. Analysis of the Images

Using DS9, we selected the target images that showed any kind of interesting structure(s). We were interested in structures, with small features, less than 5000AU, important to massive star formation (see attachments: Selected IRAS, and see: Table 5).

The size scales of the structures (in AU) were calculated using the shape drawing tool inside DS9 (Region > Shape > Circle or Line) to select part of the region we want to analyze, and a formula to convert the shape's arcsec length to the AU length. Clicking two times repeatedly in the drawn shape (or, with the shape selected, Region > Get Information) we get the length of the shape in arcsec $\theta('')$. Using the expression: $D = \frac{d \cdot \theta('')}{206265}$ (where d is the distance of the source in AU, theta the sizescale in arcsec and D is the sizescale in AU) to convert to the physical scale length or size scale, in astronomic units, we can have an idea of what the structure is. For observed structures with much less than 20 000 AU (less than 0.1pc) we have dense cores, with single sources and their environment resolved. Since these observations allowed us to probe into size scales of a few hundred AU (~700AU), we could examine the embedded stellar content and environment of some of the selected IRAS.

RAJ2000	DEJ2000	IRAS	Dist (kpc)	Lum ($L_{\odot}$)
135.47598	-47.73355	09002-4732	1.2	39000.
260.22318	-35.78349	17175-3544	1.5	78000.
238.95179	-52.71981	15520-5234	2.9	200000.
245.38538	-50.42169	16177-5018	3.4	340000.
232.33470	-56.52481	15254-5621	4.4	120000.
241.90862	-52.51430	16037-5223	4.9	110000.
197.80155	-62.57747	13079-6218	4.9	280000.
240.1367	-52.7460	15567-5236	7.0	8.0e+05

Table 5 - List of selected IRAS sources

For the selected sources (see Table 5), we have turned to SIMBAD Astronomical Database (http://simbad.u-strasbg.fr) to find the available bibliography, papers and articles, and see what has been discovered so far.

5. Notes for Individual Targets

All the information, for each selected IRAS region, was researched in the available bibliography presented in the SIMBAD Astronomical Database (http://simbad.u-strasbg.fr) and carefully gathered, with exception of the ones IRAS 16037-5223, IRAS 17175-3544 because there were no articles with conclusive and relevant data on emission lines, masers, etc.

5.1. IRAS 09002-4732

Massive star formation was inferred from the strong radio source G268.42-0.85 (Manchester & Goss 1969) which was classified later as being an ultra-compact HII region (UC HII). The luminosity, assuming the ionizing source as a single star at a distance of 1.3kpc, is 9×10^4 $L_\odot$ (see: Ghosh et al. 2000). Other evidence of massive star formation is water maser emission (see: Braz et al. 1989) and a massive molecular cloud core of $600M_\odot$ (see: Zinchenko et al. 1995) assuming a distance of 1.3 kpc.

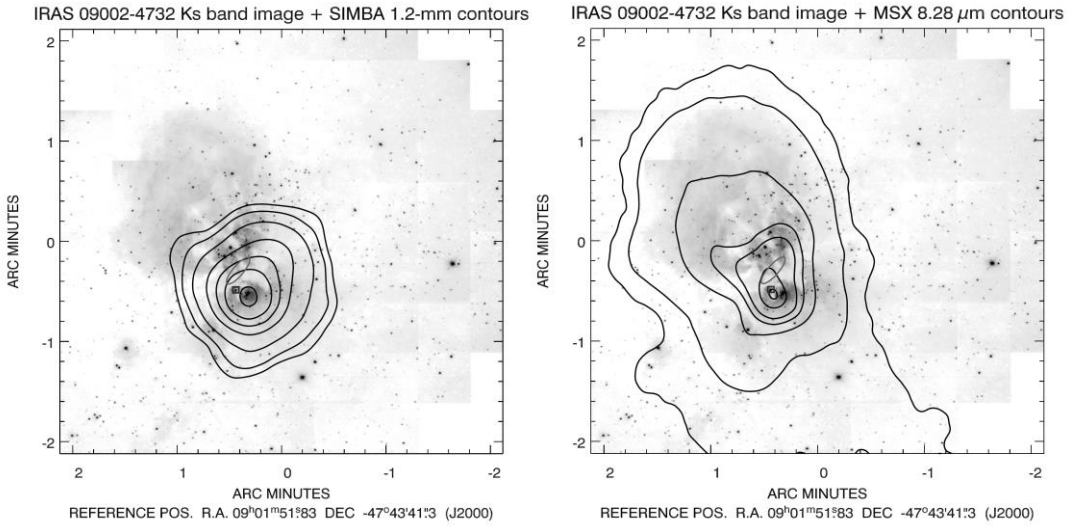

Figure 4 - Large-scale observations of IRAS 09002-4732
"Left panel: 1.2 mm SIMBA/SEST contours overlaid on the grayscale ISAAC Ks-band image. The contour levels correspond to (5, 10, 20, 40, 60, 80, 110) × 46 mJy/beam. The inverted gray scale ISAAC Ks image shows the stellar population and the short-wavelength nebulosity. Right Panel: high sensitivity MSX 8.28 μm contours, showing an extended, continuous distribution of warm dust in the star-forming region. The contours mark 5, 10, 50, 100, 150, 250, 300 σ levels; the MSX point source flux is 30.74 Jy. The square marks the radio position of the UC H II region G268.42-0.85, while the ellipse indicates the positional error ellipse of the IRAS point source 09002-4732. The MSX A-band images are probably influenced by PAH emission and this explains the offset between the IRAS- and MSX-peaks." From Apai, D., et al. 2005

There are two distinct lobes that can be seen in the large scales observation of the region IRAS 09002-4732. “A dark lane extending in east-west direction cuts across the nebula, creating the impression of bipolarity.” “These large-scale observations also show that the main heating source of the dust is located in the southern lobe. In fact, the most massive star(s), indicated by the presence of an UCH II region, is located close to both the MSX and the SIMBA peak emission”. (see: Apai, D., et al. 2005, and Figure 4). (The high resolution data was obtained with ISAAC at the VLT, and the archival MSX images and photometry from Edgan et al. 1999)

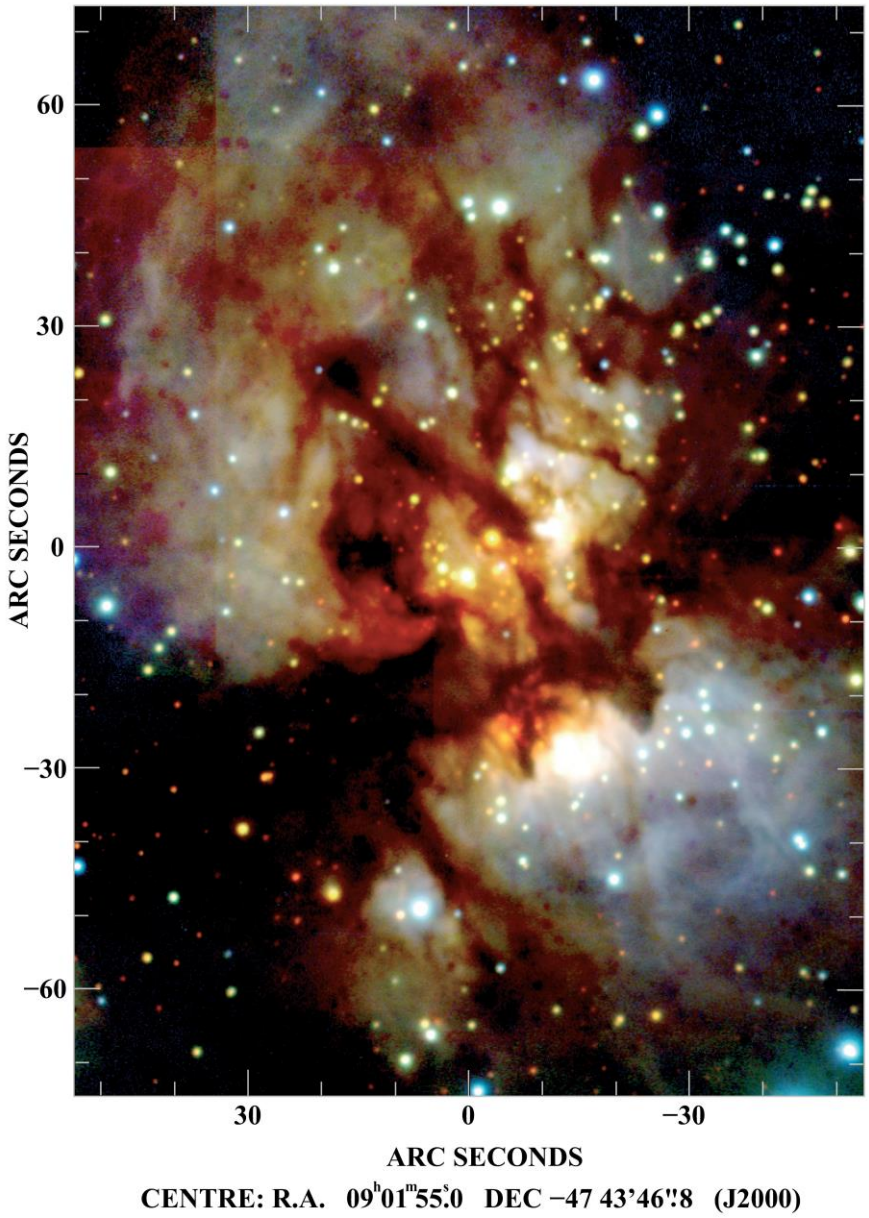

Figure 5 - Large extinction structure around IRAS 09002-4732
"False-colour composite image from the near-infrared observations. The Ks band image is coded in red, H in green and Js in blue." From Apai, D., et al. 2005

The reflection nebulosity, identified by Brand et al. 1986 (see: Brand et al. 1986), with optical and near-infrared emission (see: Figure 5), dominated by blue scattered light, south-west of the UC HII region (G268.42-0.85) has an approximately size of 1' x1'. (see: Apai, D., et al. 2005, and Figure 4) The surface brightness was plotted by Apai, D., et al. 2005 which increased towards the UC HII region, demonstrating that the source of the scattered light is nearby the UC HII region. In the southern lobe of the reflection nebulosity, the filaments density drops, a direct influence of the massive star ionizing the UCHII region. The massive star could have destroyed these structures (see: Apai, D., et al. 2005, section 3.2.2).

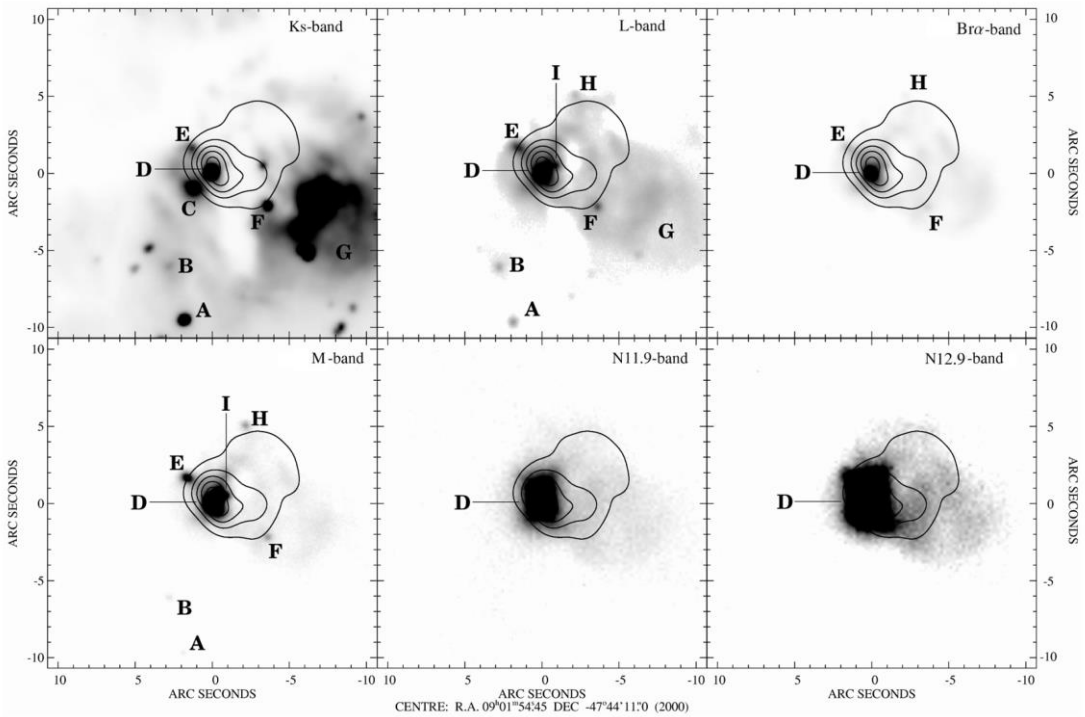

Figure 6 - Morphology of IRAS 09002-4732
"The morphology of the UC H II region G268.45-0.85 as seen in 2.2 μm (Ks), 3.78 μm (L), 4.66 μm (M), 4.07 μm (Brα), 11.9 μm (N11.9) and 12.9 μm (N12.9) images. The overlaid contours are 8.64 GHz radio continuum measurements from Walsh et al. (1998). The objects of particular interest are marked with letters from A–I."
From Apai, D., et al. 2005

About the morphology of the UC HII region, the source identified as D (see: Figure 6 and Figure 12) has good indications to be the most massive star. We have a NIR peak "coinciding with the radio peak of G268.42-0.85", emission increasing towards longer wavelengths, the most infrared excess emission, dominating at wavelengths longer than 3μm. IR emission decreases rapidly at shorter wavelengths due to high extinction (see: Apai, D., et al. 2005). The other marked sources are also good candidates for massive stars.

The UC HII region is located in the peak of the mid-infrared and the millimeter emission, as also, the reflection nebulosity. The “heating and illumination of the IRAS 09002-4732 star-forming region is dominated by the same single source or compact cluster which ionizes the UC H II region G268.42-0.85 region.” There was no other radio continuum emission found in that region, which indicates that the source identified as the most massive young star(s) is located in this region at G268.42-0.85 (see: Apai, D., et al. 2005).

This is also one of the few cases where we can find NIR and MIR emission of the ionizing source identified as D. Our image shows a better resolution of this source, but, unfortunately, this area remains unresolved even at spatial resolutions around 700AU (see: Figure 12), so we can only identify this source as a single source or a compact cluster. We could, however, compare our image, Figure 12, to the 3D Simulation, Figure 1, which has a similar scale, suggesting that we may be looking indeed to a single source, surrounded by stellar material with similar spiraling structure as seen in the simulation. The other identified sources, F for example, (Figure 6), also have the same structure. To have a better view of these sources, interferometric or spectroscopic observations are needed (see: Apai, D., et al. 2005).

5.2. IRAS 15520-5234

The MIR emission was detected in the location of the UC HII region. This region was seen at cm wavelengths (see: Ellingsen et al. 2005). The methanol masers were detected between the sources at cm continuum emission and at the strong emission from the bright mid-infrared source.

“The new observations presented here add further complexity to the knowledge of this region. The high spatial resolution mid-infrared images taken with T-ReCS (see: Figure 7) reveal a large (15×15 $arcsec^2$) extended emission region with 8 peaks (or knots)” (see: De Buizer, J. M., et al. 2009). The NACO image in Ks band (with 18×18 $arcsec^2$, see: Figure 14) also shows the peaks, along with two well defined nebular regions, UC HII regions (see: De Buizer, J. M., et al. 2009, and Ellingsen et al. 2005), near the very strong peak marked by the dashed circle.

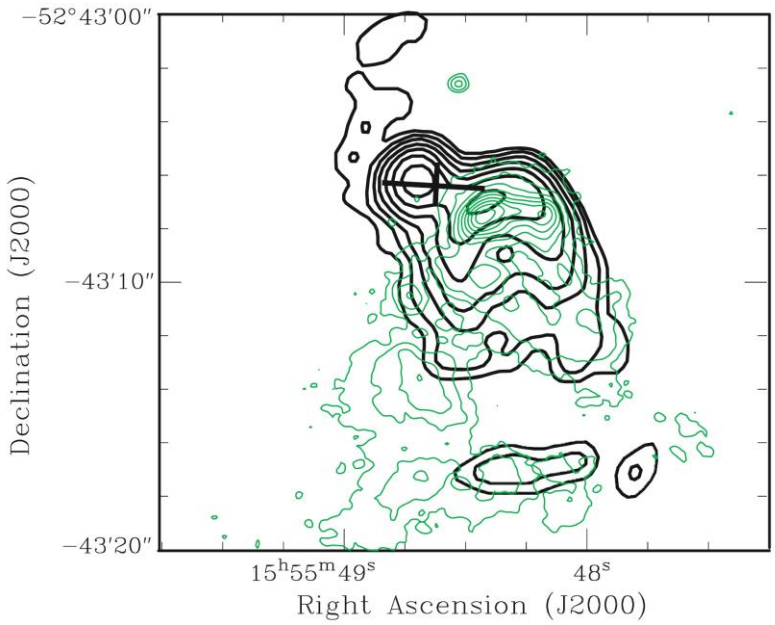

Figure 7 - IRAS 15520-5234 seen in MIR and cm continuum
"Mid-infrared T-ReCS image (green contours) and the cm continuum emission (thin black contours) “
(see: Ellingsen et al. 2005 Ellingsen et al. 2005) From De Buizer, J. M., et al. 2009

“Even with all of the complexity of this region, the SiO emission is clearly not coming from an outflow (or outflows) centered at the maser location and perpendicular to the angle of the methanol maser distribution. Consequently, these observations are inconsistent with the maser-disk hypothesis.” (see: De Buizer, J. M., et al. 2009)

Although some L band emission was detected (3.3μm, Walsh et al. 2001), it appears that there is no NIR source at the maser location (De Buizer 2003, Goedhart et al. 2002). However, there are “two UC HII regions near the maser location” (Figure 7), “one compact and round, and the other large and cometary shaped” (see: De Buizer, J. M., et al. 2009, and Ellingsen et al. 2005) (see: Figure 14).

NH3 (ammonia) emission was not detected from the UC HII regions, although it is strong at larger scales around the UC HII regions (see: Beuther, Walsh & Longmore 2009).

“We witness large-scale hot NH3 emission around G328.81+0.63 from lines with excitation temperatures as high as 295 K.” “This implies that the central formed/ forming high-mass stars have heated up significant amounts of gas out to distances exceeding 30,000 AU from the center to temperatures in excess of 100 K without yet destroying the surrounding gas envelope." (see: Beuther, Walsh & Longmore 2009)

This statement supports the theory proposed by Krumholz et al. (by Krumholz et al. 2007b) that "radiative feedback from the central protostar is able to heat up the surrounding envelope strong enough that further thermal fragmentation will be largely suppressed." (see: Beuther, Walsh & Longmore 2009)

5.3. IRAS 16177-5018

The work by Roman-Lopes et al. (2003), based on NIR-imaging photometry, showed a massive young stellar cluster, very massive, associated with an HII region. A possible luminosity, for a single star occupying this region is $2.8\times10^5\,L_\odot$, with a mass of $42M_\odot$ (see: Roman-Lopes et al. 2003).

The cluster associated to this IRAS region is part of the RCW106 complex or region. The spectrum analysis in Roman-Lopes et al. (2009) revealed emission lines, at the IRAS 16177_IRS1 (see: Figure 8), typical of very hot stars (CIV, NIII, NV respectively, 2.078μm, 2.116 μm and 2.100 μm).

Our image offers better resolution of the IRAS 16177_IRS1 and it clearly shows 3 distinct sources located in the HII region, one having a stronger peak marked by the dashed circle (see: Figure 15), that could be the most massive star, in case of a single source.

“We also detected in the associated nebular Kband spectrum, the s-process [KrIII] and [SeIV] high excitation emission lines, previously identified only in planetary nebula.” (see: Roman-Lopes et al. 2009) If an HII region is considered, these lines may be produced by an O star ionizing the high density environment, a case very similar to those discussed above.

The "measured HeI 2.113/Brγ ratio indicate the presence of an exciting star whose Teff is greater than 40,000 K. This would correspond to a single star of spectral type earlier than O5v, or O4.5iii, or O4i, depending on the luminosity class.” Based on the data by Roman-Lopes et al. (2009), this may be a region where very hot stars are still being formed.

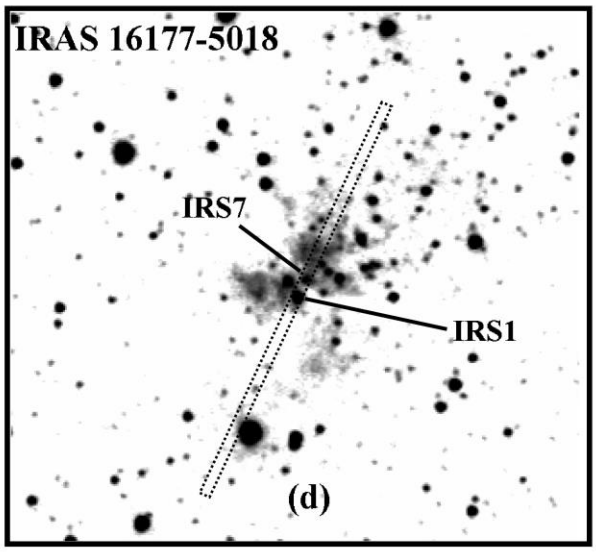

Figure 8 - NIR survey of IRAS16177-5018
Panel has the size of 2'× 2.5'. North is to the top, east to the left. "In each cluster, we indicate the slit position (dotted lines) and the sources for which we obtained K band GNIRS spectra." From Roman-Lopes et al. 2009

Other source, denoted by IRS7 (see: Figure 8, and Roman-Lopes et al. 2009), who's spectrum is typical of an YSO (see: Roman-Lopes et al. 2003) has an HeI (2.058 μm) emission line that "shows a P-Cygni profile that may indicate the presence of expanding motion. High resolution radio observations would be useful to clarify this issue." (see: Figure 8, and Roman-Lopes et al. 2009).

5.4. IRAS 15254-5621

The analysis of the spectrum by Araya et al. (2005), revealed "blue and red line wings in all observed CS and 13CO transitions" indicating a possible existence of molecular outflows from YSO. The use of a population diagram to obtain a CH3CN rotation temperature showed a data distribution indicating a two-temperature profile, rather than a one-temperature profile. The temperature of the cold component is around 30-42 K, typical of molecular gas around UC HII regions (see: Hofner et al. 2000), and the temperature of the hot component was greater than 90 K (see: Araya et al. 2005). The source may be surrounded by a very dense environment, located in a high massive compact HII region.

Our image by NACO in Ks band (see: Figure 16) shows a strong peak surrounded by a nebular region, possibly an UC HII region, with the size of 0.1' (other sources are also present in this region). Due to the size and shape of the peak/region marked by the dashed circle it may be a compact cluster (see: Figure 16).

Was detected CH3CN, OH, and H2O maser emissions and an unresolved radio continuum source, less than 2'', in the IRAS 15254-5621 (see: Araya et al. 2005,

Walsh et al. 1998, Chan et al. 1996). Broad radio recombination lines “suggest that the unresolved radio continuum source might be an HC HII region”. “It is thought that HCH II regions are precursors of the UCH II region phase (e.g., Sewilo et al. 2004), thus, IRAS 15254-5621 is likely to be a quite young region of massive star formation. The luminosity from this region is equivalent to an O6 (ZAMS) star (see: Walsh et al. 1997).” (see: Araya et al. 2005)

5.5. IRAS 13079-6218

There are several masers detected, H2O, OH and methanol, in the location of the HII region, [CH87] 305.254+0.204, in this IRAS (see: Clark and Porter 2004, Beuther, Walsh & Longmore 2009). According to Walsh et al. (1997) methanol maser emission is a good indicator of high mass star forming regions, since it has been detected in known regions of intense star formation. The detection of SiO emission is also explained as an evidence for star formation, “thought to occur behind shocks driven by energetic outflows from young stellar objects” (see: Clark and Porter 2004). These are great indicators of massive star formation taking place in the location of this IRAS.

Since the region is crowded with sources, an attempt to determine the bolometric luminosity using integrated IR fluxes will “lead to overestimates for the bolometric luminosity of “individual” sources” (see: Clark and Porter 2004). A high spatial resolution of this region showed several objects (see: Walsh et al. 2001, Figure 9).

Also, by observing IRAS 13079–6218 in Ks band (see: Figure 18) we can see several sources, possible massive stars in formation (that couldn’t be seen in Figure 9) in the location of the HII region.

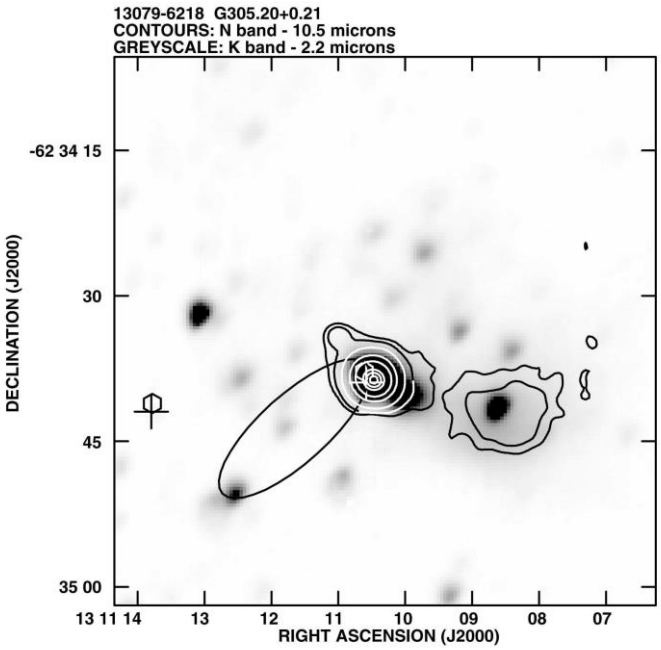

Figure 9 - High Spatial Resolution of IRAS13079-6218
IRAS 13079–6218 also known as G305:20 1 0:21. "Source 27 is in the centre of the image, source 28 is to the west and source 29 is the maser site to the east. The positions of the methanol maser sites are adopted from Norris et al. (1993). An artifact of an internal reflection in MANIAC can be seen 5 arcsec to the north-east of the main, unresolved MIR source, and is thus not an astrophysical object." From Walsh et al. 2001.

The fluxes of the UC HII region points out the formation of an OB population of stars in this region of the nebula. Significant amount of radio emission was also found to be coincident with this MIR nebula, that looks like to be one of the most massive star forming regions found in our galaxy (see: Clark and Porter 2004).

Besides the methanol maser emission, high-excitation NH_3 (ammonium) lines can also be good tracers of the very dense and hot environment of YSO in formation. Position-velocity diagrams of the NH_3 (4,4) and (5,5) lines, in Beuther, Walsh & Longmore (2009), showing the velocity gradient, may indicate that the "NH_3 structure corresponds to a large rotating and infalling envelope that may feed a real Keplerian accretion disk at its center." "Although the spatial resolution is of order a few 1000 AU, we do not identify obvious Keplerian signatures". (see: Beuther, Walsh & Longmore 2009)

The detection of disks in IR is made by measuring the excess emission of the spectral energy distribution (SED) using multiple IR photometry, but an alternate method would be by analyzing images, in case of having MIR images at wavelengths longer than 12μm, due to the thermal dust emission, which can be seen.

In addition, the work by De Buizer (2003) also contains some interesting information regarding the IRAS 13079–6218 (G305.21+0.21). Very bright NIR source surrounded

by extended emission, also mentioned in Walsh et al. (1999) and found to be coincident with the maser location (see: De Buizer et al. 2000).

The extended NIR emission seems to come from a large HII region that can also be seen in the MIR (see: De Buizer et al. 2000, Walsh et al. 2001, and Figure 10).

The work presented by De Buizer (2003) “is the first to seemingly contradict the hypotheses that linearly distributed methanol masers are generally found in circumstellar disks.” (see: De Buizer 2003)

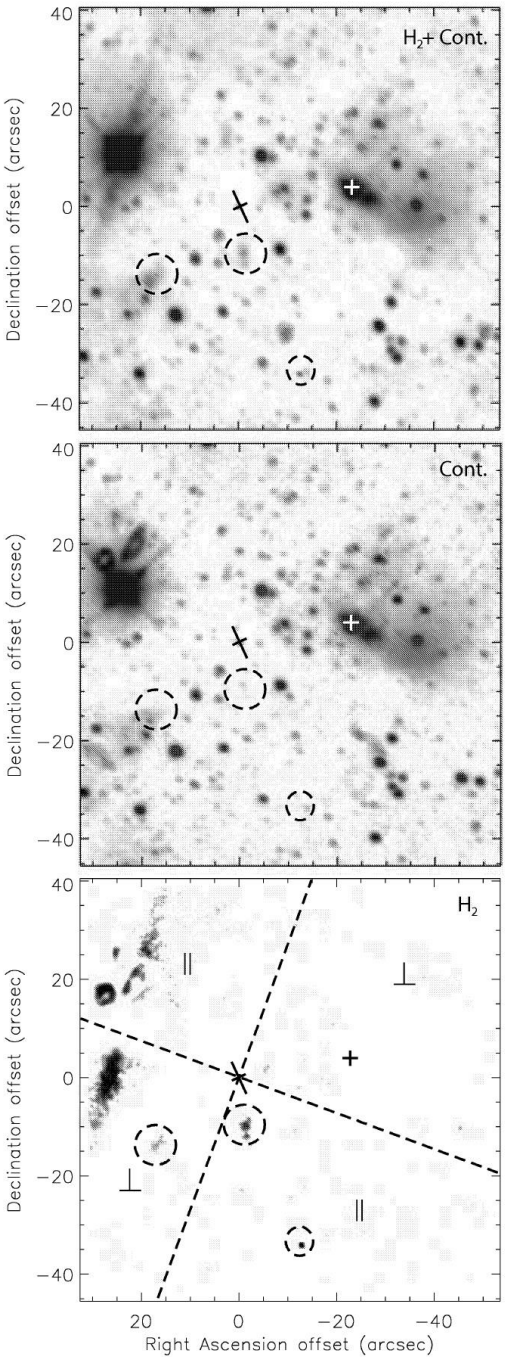

Figure 10 - H_2+Continuum of IRAS 13079–6218 (G305.21+0.21)
"H2+continuum, continuum and residual H2 images. Crosses represent maser group locations, and elongated axes show the position angle of linear maser distributions. Dashed ellipses encompass areas of H2 emission. Dashed lines in the H2 images devide the frame into quadrants parallel to and perpendicular to the maser position angle. All emission in the upper left-hand corner of the H2 image is "noise" caused by the bright stellar source there."
From De Buizer 2003.

5.6. IRAS 15567-5236

The IRAS 15567-5236 (G329.34+0.15) is identified as a cometary compact HII region, due to the strong radio emission detection (see: Walsh et al. 1998, Peeters et al. 2005), at an heliocentric distance of 7.8 (near) or 9.6kpc (far) (see: Walsh et al. 1997). Methanol masers were detected and associated with this IRAS (see: Figure 11, Ellingsen et al. 1996, Walsh et al. 1998, and Pestalozzi et al. 2002).

The morphology of this region is better shown in our NACO image (Figure 19), where the strong emission can be resolved into a distinct source (seen in KS band) surrounded by a nebula, UC HII region. This source marked by the dashed circle and with the size of 0.2'' may be a very massive star. Considering that we have a single star ionizing the surrounding material, and producing the FIR radiation observed, the star's spectral type is less than O4 (see: Peeters et al. 2005).

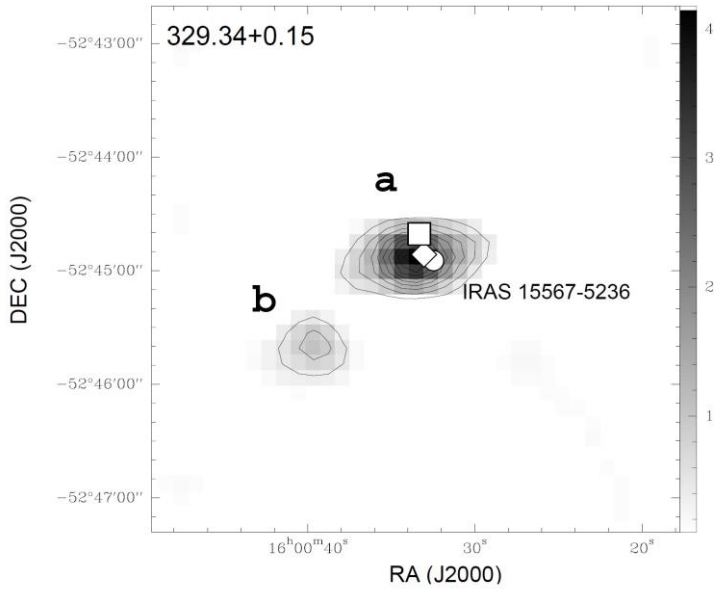

Figure 11 - Maser emission of IRAS 15567-5236 (G329.34+0.15)
SIMBA map of the observed methanol maser source
From Pestalozzi et al. 2002

"The colours of IRAS 15567-5236 suggest that we are observing a young object with very low optical depth ($\tau_\upsilon < 0.1$)" (see: Pestalozzi et al. 2002).

6. Conclusions

21 IRAS sources were observed using AO data of which eight sources showed unresolved point like objects, with interesting structures. Based on the information found, and also on the analysis of the images using IRAF and DS9, these sources (see: Table 5) are good candidates of massive young stars. Some of these objects are also surrounded by faint point sources indicating clustering. They are found in UC HII regions (regions of ionized gas due to the radiation coming from the stellar core or compact cluster in some cases) located inside high density cores (< 0.1pc in diameter), with characteristics of YSOs (see: Roman-Lopes et al. 2003) and often associated with maser emission (CH3OH, NH3, H2O, OH).

The observations allowed to probe into size scales of ~1000 AU. But even with that spatial resolution, the best we've got so far, the sources remain unresolved.

Some of the targets are crowded with multiple sources, so the bolometric luminosities of individual objects (calculated from IR fluxes) will be overestimated due to contamination from the other sources. Nevertheless, most of the values can be interpreted as an upper limit for the real value, leading to the conclusion that formation of a population of OB stars is occurring in a number of selected targets. This complies with the detected fluxes of HII regions (see: Clark and Porter 2004).

References

Apai, D., et al. 2005, in Infrared portrait of the nearby massive star-forming region IRAS 09002-4732, Apai, D.; Linz, H.; Henning, Th.; Stecklum, B., Astronomy and Astrophysics, Vol 434, Issue 3, pp.987-1003, 2005 ..... 25, 26, 27, 28

Araya et al. 2005, in CH3CN Observations toward Southern Massive Star-forming Regions, Araya, Esteban; Hofner, Peter; Kurtz, Stan; Bronfman, Leonardo; DeDeo, Simon, The Astrophysical Journal Supplement Series, Vol157, Issue 2, pp. 279-301, 2005 ..... 31, 32

Bally 2002, in Hot Star Workshop III: The Earliest Stages of Massive Star Birth, J. Bally, ASP Conference Proceedings, Vol. 267. Edited by Paul A. Crowther. 2002, p. 219 8

Beuther, Walsh & Longmore 2009, in Hot high-mass accretion disk candidates, Beuther, H., Walsh, A.J., and Longmore, S.N., Astrophysical Journal Supplement Series 2009, 184 (2). pp. 366-386 ..... 29, 32, 33

Bodenheimer, P. H., 2011, in Principles of Star Formation, P.H. Bodenheimer, Astronomy and Astrophysics Library, Springer 2011 ..... 2, 3, 5, 7, 9, 10

Bonnell, I. A., & Bate, M. R. 2006, MNRAS, 370, 488 9

Bonnell, I. A., Bate, M. R., & Zinnecker, H. 1998, MNRAS, 298, 93 9

Bonnell, I. A., Bate, M. R., Clarke, C. J., & Pringle, J. E. 2001, MNRAS, 323, 785 9

Born, M., Wolf, E., 1999, in Principles of Optics, 7th ed, M. Born and E. Wolf, New York: Cambridge UP, 1999 13

Brand et al. 1986, Brand, J., Blitz, L., & Wouterloot, J. G. A. 1986, Astronomy and Astrophysics Supplement, 65, 537 27

Braz et al. 1989, Braz, M. A., Gregorio Hetem, J. C., Scalise, E., Monteiro Do Vale, J. L., & Gaylard, M. 1989, Astronomy and Astrophysics Supplement, 77, 465 25

Chan et al. 1996, Chan, S. J., Henning, Th., & Schreyer, K. 1996, Astronomy and Astrophysics Supplement, 115, 285 32

Clark and Porter 2004, in Triggered massive star formation in the vicinity of WR 48a, Clark, James and Porter, J. M., 2004, Astronomy and Astrophysics, 427(3), pp. 839–847 ..... 32, 33, 37

Cunningham et al. 2011, in Radiation-hydrodynamic Simulations of Massive Star Formation with Protostellar Outflows, Cunningham, Andrew J.; Klein, Richard I.; Krumholz, Mark R.; McKee, Christopher F., The Astrophysical Journal, Vol 740, Issue 2, article id. 107, 18 pp. 2011 2

De Buizer 2003, De Buizer, J. M. 2003, MNRAS, 341, 277 ..... 29, 33, 34, 35, 36

De Buizer et al. 2000, in Mid-Infrared Imaging of Star-forming Regions Containing Methanol Masers, De Buizer, James M.; Piña, Robert K.; Telesco, Charles M., 2000, The Astrophysical Journal Supplement Series, Vol 130, Issue 2, pp. 437-461 34

De Buizer, J. M., et al. 2009, in SiO Outflow Signatures Toward Massive Young Stellar Objects with Linearly Distributed Methanol Masers, De Buizer, J.M., Redman, R., Longmore, S.N., Caswell, J., & Feldman, P., Astronomy & Astrophysics 2009, 493, p. 127-143 .....9, 11, 28, 29

Edgan et al. 1999, Egan, M. P., Price, S. D., Moshir, M. M., et al. 1999, MSX5C Infrared Point Source Catalog, Tech. Rep., Air Force Research Lab., AFRL-VS-TR-1999-1522 26

Ellingsen 2006, in Methanol masers: Reliable tracers of the early stages of high-mass star formation, Ellingsen, S. P., The Astrophysical Journal, vol 638, p.241, 2006 11

Ellingsen et al. 1996, in A survey of the Galactic plane for 6.7-GHz methanol masers - I. l=325 deg-335 deg b=-0.˚53-0.˚53, Ellingsen, S. P.; von Bibra, M. L.; McCulloch, P. M.; Norris, R. P.; Deshpande, A. A.; Phillips, C. J., 1996, Monthly Notices of the Royal Astronomical Society, Vol 280, Issue 2, pp. 378-396 36

Ellingsen et al. 2005, Ellingsen, S. P., Shabala, S. S., & Kurtz, S. E. 2005, MNRAS, 357, 1003 .....28, 29

Faúndez et al., 2004, in SIMBA survey of southern high-mass star forming regions. I. Physical parameters of the 1.2 mm/IRAS sources, Faúndez, S., Bronfman, L., Garay, G., Chini, R., Nyman, L.-A., May, Astronomy and Astrophysics, vol 426, p. 97–103, 2004 .....3, 16

Garay, G., Lizano, S. 1999, in Massive Stars: Their Environment and Formation, ed. Guido Garay & Susana Lizano, Publications of the Astronomical Society of the Pacific, Vol. 111, No. 763, 1999, p. 1049-1087.....8, 10

Ghosh et al. 2000, Ghosh, S. K., Mookerjea, B., Rengarajan, T. N., Tandon, S. N., & Verma, R. P. 2000, Astronomy and Astrophysics, 363, 744..... 25

Goedhart et al. 2002, Goedhart, S., van der Walt, D. J., & Gaylard, M. J. 2002, MNRAS, 335, 125 29

Hoare, M. G. et al. 2006, in Ultra-Compact HII Regions and the Early Lives of Massive Stars, M. G. Hoare, S. E. Kurtz, S. Lizano, E. Keto, P. Hofner, astro-ph/0603560, 2006 8

Hofner et al. 2000, Hofner, P., Wyrowski, F., Walmsley, C. M., & Churchwell, E. 2000, The Astrophysical Journal, 536, 393..... 31

Krumholz et al. 2005b, in How Protostellar Outflows Help Massive Stars Form, Krumholz, Mark R.; McKee, Christopher F.; Klein, Richard I., The Astrophysical Journal, Vol 618, Issue 1, pp. L33-L36, 2005 9

Krumholz et al. 2005c, The formation of stars by gravitational collapse rather than competitive accretion, Krumholz, Mark R.; McKee, Christopher F.; Klein, Richard I, Nature, Volume 438, Issue 7066, pp. 332-334, 2005..... 9

Krumholz et al. 2007b, in Radiation-Hydrodynamic Simulations of Collapse and Fragmentation in Massive Protostellar Cores, Krumholz, M. R., Klein, R. I., & McKee, C. F. 2007b, The Astrophysical Journal, 656, 959 29

Krumholz et al. 2009, in The Formation of Massive Star Systems by Accretion, Mark R. Krumholz, Richard I. Klein, Christopher F. McKee, Stella S. R. Offner, Andrew J. Cunningham, Science 2009.....2, 10

Kuiper et al. 2012, On the stability of radiation-pressure-dominated cavities, R. Kuiper, H. Klahr, H. Beuther, Th. Henning, A&A 537 2

Kutner, M. L., 2003, in Astronomy: A Physical Perspective, 2nd ed, Kutner, M. L., Cambridge University Press, 2003, p.280..... 13

Lada, C.J., Lada, E.A., 2003, in Embedded Clusters in Molecular Clouds, Lada, Charles J.; Lada, Elizabeth A., Annual Review of Astronomy and Astrophysics, vol. 41, pp.57-115, 2003 2

Manchester & Goss 1969, Manchester, B. A., & Goss, W. M., Australian Journal of Physics, Astrophysical Supplement, 11, 35, 1969 25

McKee & Tan 2002, in Massive star formation in 100,000 years from turbulent and pressurized molecular clouds, McKee, Christopher F.; Tan, Jonathan C., Nature, Volume 416, Issue 6876, pp. 59-61, 2002 9

McKee & Tan 2003, in The Formation of Massive Stars from Turbulent Cores, McKee, Christopher F.; Tan, Jonathan C., The Astrophysical Journal Volume 585, Issue 2, pp. 850-871, 2003 9

Minier et al. 2003, in The protostellar mass limit for 6.7 GHz methanol masers - I. A low-mass YSO surveyMinier, V., Ellingsen, S. P., Norris, R. P., & Booth, R. S., Astronomy & Astrophysics, 403, p.1095, 2003 11

Norris et al. 1998, in Methanol Masers as Tracers of Circumstellar Disks, R. P. Norris, S. E. Byleveld, P. J. Diamond, S. P. Ellingsen, R. H. Ferris, R. G. Gough, M. J. Kesteven, P. M. McCulloch, C. J. Phillips, J. E. Reynolds, A. K. Tzioumis, Y. Takahashi, E. R. Troup, and K. J. Wellington, The Astrophysical Journal, Vol 508, 275, 1998 11

Peeters et al. 2005, in The Prominent Dust Emission Feature near 8.9 μm in Four H II Regions, Peeters, E.; Tielens, A. G. G. M.; Boogert, A. C. A.; Hayward, T. L.;

Allamandola, L. J., 2005, The Astrophysical Journal, Vol 620, Issue 2, pp. 774-785 36

Pestalozzi et al. 2002, in First SIMBA observations towards CH3OH masers, M. Pestalozzi, E. M. L. Humphreys, and R. S. Booth, 2002, Astronomy & Astrophysics, Vol 384, Issue 2, pp. L15-L18..... 36

Roman-Lopes et al. 2003, in Discovery of a Young Massive Stellar Cluster Associated with IRAS Source 16177−5018, A. Roman-Lopes, Z. Abraham, and J. R. D. Lépine, The Astronomical Journal, vol 126, p.1896, 2003 .....11, 30, 31, 37

Roman-Lopes et al. 2009, in GEMINI near-infrared spectroscopic observations of young massive stars embedded in molecular clouds, A. Roman-Lopes, Z. Abraham, R. Ortiz, A. Rodrigues-Ardila, 2009, Monthly Notices of the Royal Astronomical Society , 394, 467-478 .....30, 31

Salaris, M., Cassisi, S., 2005, in Evolution of stars and stellar populations, Maurizio Salaris; Santi Cassisi, John Wiley & Sons, 2005, p. 138-140..... 5

Sewilo et al. 2004, Sewilo, M., Churchwell, E., Kurtz, S., Goss, W. M., & Hofner, P. 2004, The Astrophysical Journal, 605, 285..... 32

Shu, F. H. 1982, in The Physical Universe, Frank H. Shu, University Science Books, 1982, p. 146 5

Stahler et al. 2000, in Protostars and Planets IV (V. Mannings et al., eds), Stahler, S. W., Palla, F., and Ho, P. T. P, Tucson: University of Arizona Press 2000, pp 327-51..... 8

Walsh et al. 1997, Walsh, A. J., Hyland, A. R., Robinson, G., & Burton, M. G. 1997, MNRAS, 291, 261 .....32, 36

Walsh et al. 1998, in Studies of ultracompact HII regions - II. High-resolution radio continuum and methanol maser survey, Walsh, A. J., Burton, M. G., Hyland, A. R., & Robinson, G., Monthly Notices of the Royal Astronomical Society, Volume 301, Issue 3, pp. 640-698, 1998.....11, 32, 36

Walsh et al. 1998, in Studies of ultracompact HII regions - III. Near-infrared survey of selected regions, Walsh, A. J., Burton, M. G., Hyland, A. R., & Robinson, G., Monthly Notices of the Royal Astronomical Society, Volume 309, Issue 4, pp. 905-922, 1999 34

Walsh et al. 2001, Walsh, A. J., Bertoldi, F., Burton, M. G., & Nikola, T. 2001, MNRAS, 326, 36 ..... 29, 32, 33, 34, 35, 36

Walsh et al. 2003, in Observations of warm dust near methanol masers, Walsh, A. J., Macdonald, G. H., Alvey, N. D. S., Burton, M. G., & Lee, J.-K., Astronomy & Astrophysics, 410, p.597-610, 2003 11

Wood & Churchwell 1989, Wood, D.O.S., Churchwell, E. 1989, The Astrophysical Journal, vol 340, p.265, 1989 11

Yorke & Sonnhalter 2002, ApJ, 569, 846 Yorke H., Sonnhalter C 2002, in On the Formation of Massive Stars, Yorke, H. W. & Sonnhalter. C., The Astrophysical Journal, 569:846-862 2002..... 8

Zinchenko et al. 1995, Zinchenko, I., Mattila, K., & Toriseva, M. 1995, Astronomy and Astrophysics Supplement, 111, 95 25

Websites:

Adaptive Optics technique:

http://www.astro.caltech.edu/palomar/AO

ESO Archive Query Form:

http://archive.eso.org/eso/eso_archive_main.html

IRAF:

http://iraf.noao.edu

SAOImage DS9:

http://hea-www.harvard.edu/RD/ds9/site/Home.html

SIMBAD Astronomical Database:

http://simbad.u-strasbg.fr

Stars spectral type characteristics:

http://en.wikipedia.org/wiki/Stellar_classification

http://www.uni.edu/morgans/astro/course/Notes/section2/spectraltemps.html

MS Stars, Evolution:

http://spiff.rit.edu/classes/phys230/lectures/star_age/star_age.html

VLT/NACO instrument:

http://www.eso.org/sci/facilities/paranal/instruments/naco

Attachments

Selected IRAS

The dashed circle indicates the most luminous point like objects.

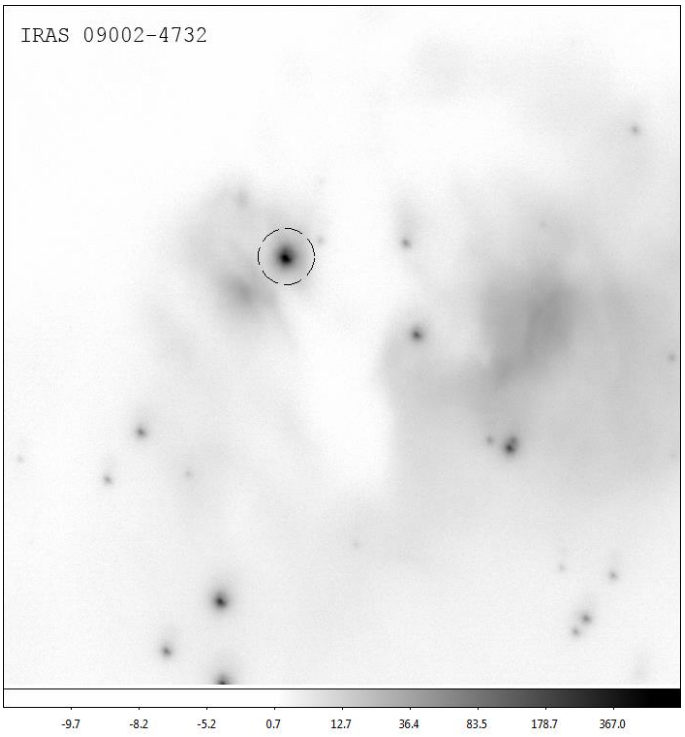

Figure 12 - IRAS 09002-4732 (in Ks band)
Panel has the size of 0.3' x 0.3'. Dashed circle has the radius of 0.8'' approx (1000 AU).

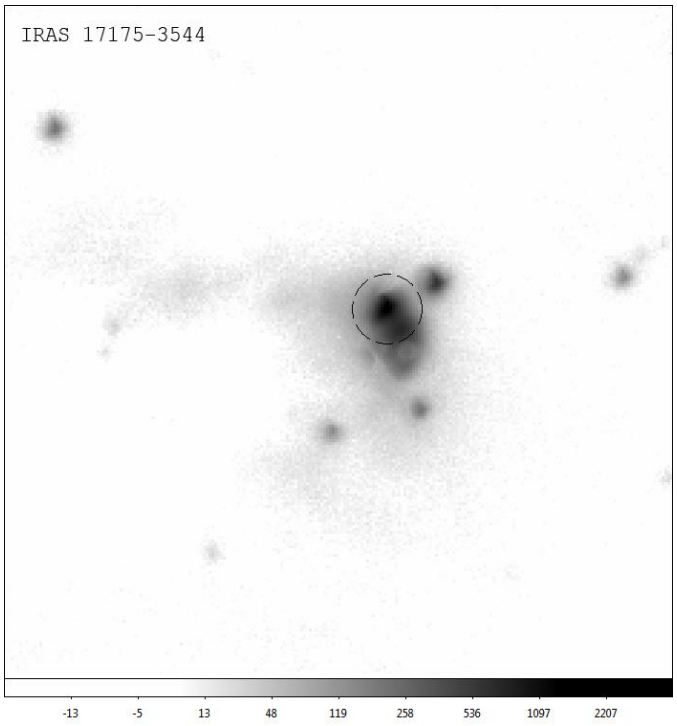

Figure 13 - IRAS 17175-3544 (in Ks band)
Panel has the size of 0.2' x 0.2'. Dashed circle has the radius of 0.67'' approx (1000 AU).

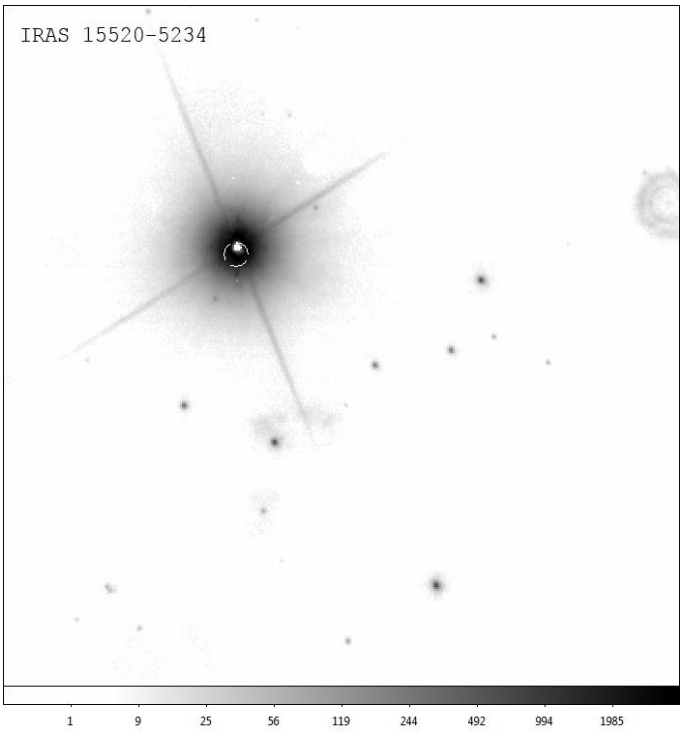

Figure 14 - IRAS 15520-5234 (in Ks band)
Panel has the size of 0.3' x 0.3'. Dashed circle has the radius of 0.35'' approx (1000 AU).

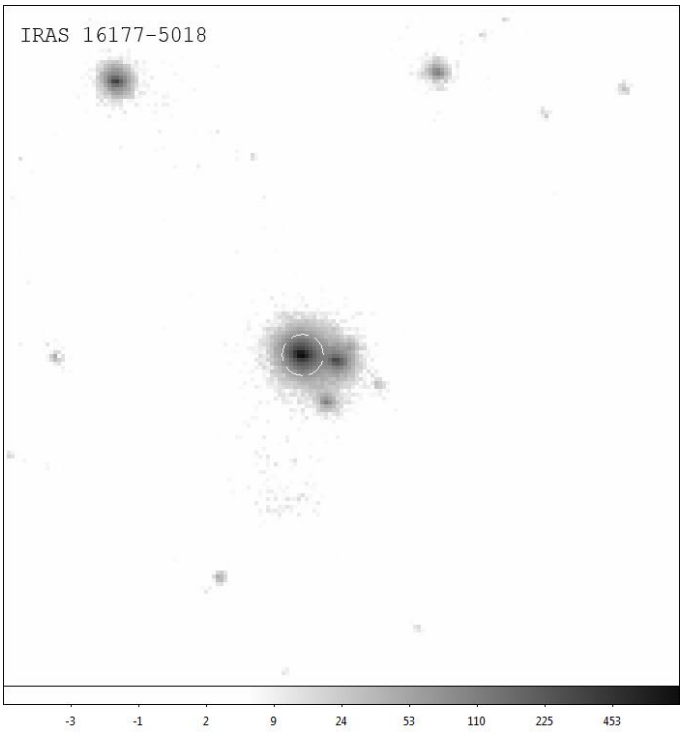

Figure 15 - IRAS 16177-5018 (in Ks band)
Panel has the size of 0.15' x 0.15'. Dashed circle has the radius of 0.3'' approx (1000 AU).

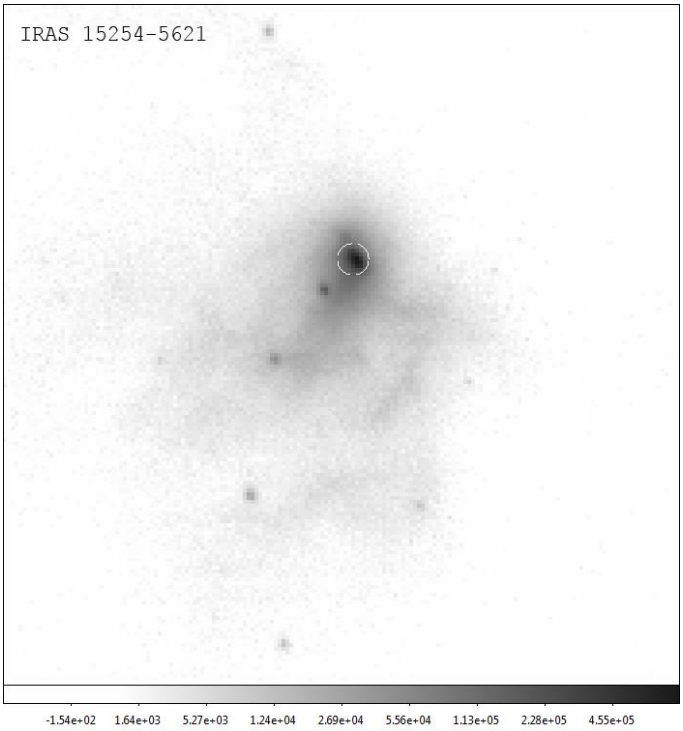

Figure 16 - IRAS 15254-5621 (in Ks band)
Panel has the size of 0.15' x 0.15'. Dashed circle has the radius of 0.2'' approx (1000 AU).

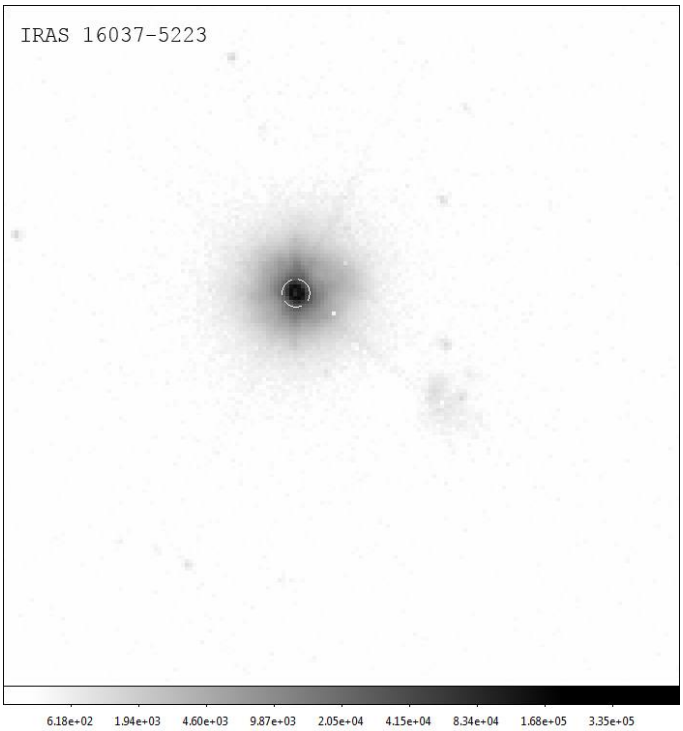

Figure 17 - IRAS 16037-5223 (in Ks band)
Panel has the size of 0.15' x 0.15'. Dashed circle has the radius of 0.2'' approx (1000 AU).

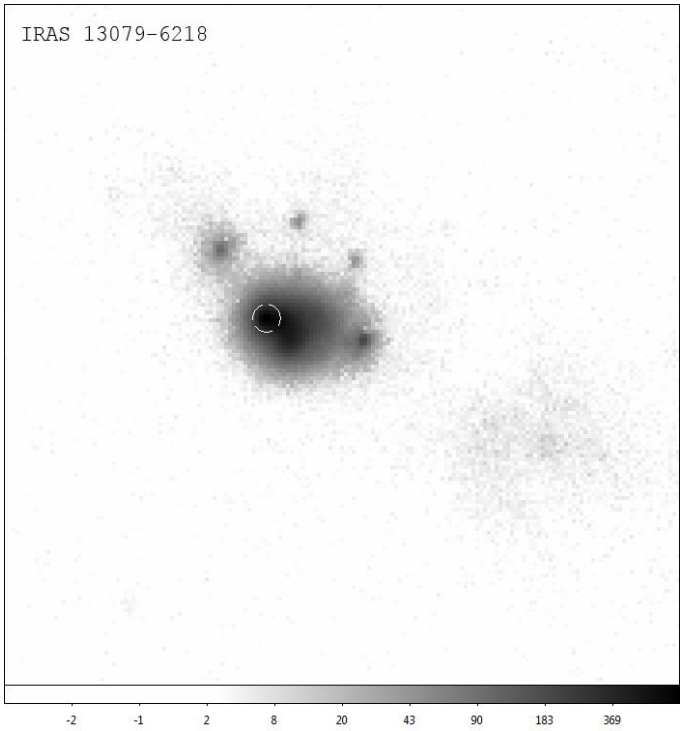

Figure 18 - IRAS 13079-6218 (in Ks band)
Panel has the size of 0.15' x 0.15'. Dashed circle has the radius of 0.2'' approx (1000 AU).

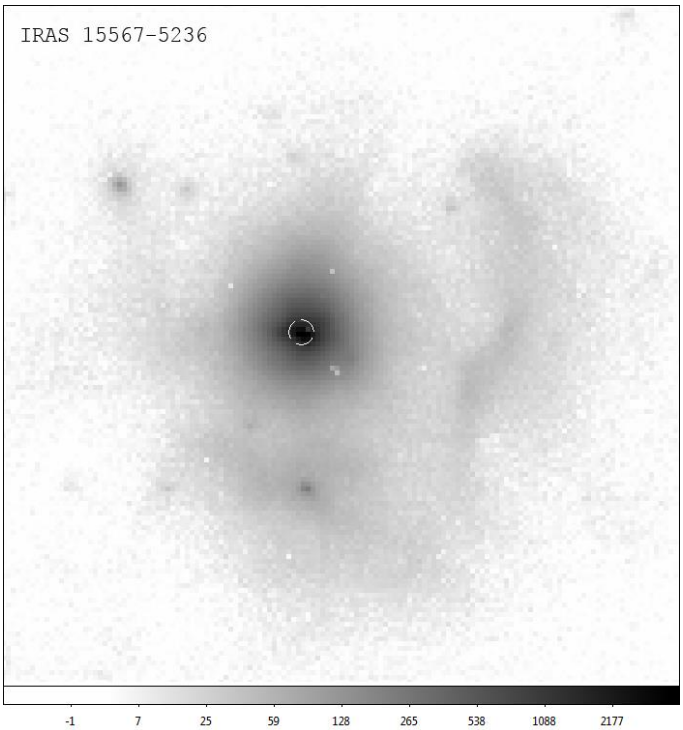

Figure 19 - IRAS 15567-5236 (in Ks band)
Panel has the size of 0.12' x 0.12'. Dashed circle has the radius of 0.1'' approx (1000 AU).